Fluid Phase Equilibria 578 (2024) 113991

Contents lists available at ScienceDirect

Fluid Phase Equilibria

journal homepage: www.sciencedirect.com/journal/fluid-phase-equilibria

Unified flash calculations with isenthalpic and isochoric constraints

V. Lipovac *, O. Duran, E. Keilegavlen, F.A. Radu, I. Berre

Center for Modeling of Coupled Subsurface Dynamics, Department of Mathematics, University of Bergen, Allégaten 41, Bergen, 5020, Norway

ARTICLE INFO

Dataset link: https://doi.org/10.5281/zenodo.8273367

Keywords:
Phase equilibrium
Unified formulation
Equation of state
Isenthalpic
Isochoric

ABSTRACT

In the unified flash procedure, a persistent set of unknowns and equations are solved in equilibrium calculations, allowing for simultaneous phase stability and split calculations. For fluids in a subcritical thermodynamic state characterized by pressure and temperature, modeling both liquid and gas phases with inequality conditions for phase fractions has been shown to incorporate the tangent-plane criterion and results in a consistent formulation of compositions for both present and absent phases. However, applications such as high-enthalpy systems in subsurface flow require a state definition using other state variables than pressure and temperature, as well as the capability to represent supercritical phases. Furthermore, the robustness of the flash across a wide range of state values is required if equilibrium dynamics are to be included in a flow and transport problem.

This work introduces constraints in terms of enthalpy and volume to allow pressure and temperature to vary in the unified setting. The constraints are shown to arise from equilibrium conditions for the relevant state functions to be minimized. To increase the range of applicability, a modified extension procedure for the compressibility factor was devised, as well as procedures for the flash initialization.

The unified formulation is extendable to allow isenthalpic and isochoric flash calculations. The initialization was devised using methodologies from the negative flash and Rachford–Rice equations. Extensive numerical tests with multiple equilibrium definitions in terms of state variables were performed. Gas–liquid, binary and a multicomponent mixture using Peng–Robinson EoS showed consistency of results which are verified using third-party code.

1. Introduction

There is a wide variety of formulations and computational methodologies for computing fluid phase equilibrium, which emphasizes the importance of identifying efficient solutions for this highly nonlinear problem. Fixing the state of a fluid mixture in terms of its intensive properties pressure, temperature and moles finds the widest range of applications in engineering. This formulation is of limited use though when facing e.g., the narrow-boiling problem [1,2] or unsteady states in fixed volumes [3]. A brief overview of the variety of formulations and their applications is found in [4]. Currently, the most widely used methodology relies on separate phase stability checks and phase-split calculations proposed by Michelsen [5,6]. This approach has in general led to numerical solution strategies of high complexity and provided the basis for many to explore different combinations of nested algorithms [1,2,7–9].

An alternative strategy for equilibrium calculations, denoted the unified formulation, was proposed by Lauser et al. [10] and considers a persistent set of unknowns and equations. A significant advantage of the unified formulation is its indirect inclusion of the tangent-plane criterion, proven by Ben Gharbia et al. [11]. No phase stability calculations have to be performed and the number of anticipated phases is defined beforehand. Variables are declared initially and no variable switching is required since vanishing variables are legitimized and assigned a mathematical meaning. The question of how to evaluate and interpret the properties of an absent phase was solved by providing extended compressibility factors for missing solutions to e.g., the cubic Peng–Robinson's equation of state [12]. Though there are earlier works using the minimization problem with Lagrange multipliers to solve issues of phase appearance and disappearance [13], it is the introduction of complementarity conditions and the analytic justification which lay the physical and mathematical foundation for the unified procedure.

Our motivation for extending and utilizing the unified formulation is its intuitive compatibility with other physical processes. In subsurface

* Corresponding author.
E-mail addresses: veljko.lipovac@uib.no (V. Lipovac), omar.duran@uib.no (O. Duran), eirik.keilegavlen@uib.no (E. Keilegavlen), florin.radu@uib.no (F.A. Radu), inga.berre@uib.no (I. Berre).
URL: https://www.uib.no/en/vista-csd (I. Berre).

https://doi.org/10.1016/j.fluid.2023.113991
Received 23 August 2023; Received in revised form 22 October 2023; Accepted 14 November 2023
Available online 17 November 2023

applications such as reservoir engineering and geothermal energy extraction, the fluid phase behavior plays a crucial role in understanding the subsurface flow. The unified formulation as a local equilibrium problem can be combined with the global flow and transport problem and allows the modeler to state the coupled physics as a closed system of equations [10]. The concept of flow and transport can be described as the propagation of the thermodynamic state of a fluid in terms of pressure, mass, and energy. The phase equilibrium problem in return is a local alteration of flow properties such as saturation, viscosity and phase mobility in general. The multitude of physical phenomena in the subsurface demands a great deal of flexibility and robustness from the flash. Finding a universal formulation which is capable of properly reflecting rapid changes in pressure, temperature or volume is, therefore, of great importance.

In this work, the phase equilibrium problem in the unified formulation, in short *unified flash*, is generalized to include specifications in terms of thermodynamic state functions other than pressure and temperature (Section 2). An equality constraint for the enthalpy or internal energy is introduced when the temperature of the mixture is unknown at equilibrium (Sections 2.2.1 and 2.2.3). Analogously, a constraint to the volume is introduced if the pressure is unknown (Section 2.2.2). Phase stability checks are included by establishing a connection to the Gibbs energy and the results provided by Ben Gharbia et al. [11]. This allows not only the unified treatment of phase-split and stability calculations using complementarity conditions, but also a general structure of the unified flash using the state function based approach (Section 2.3). A non-parametric interior-point method is introduced in Section 3 for addressing the resulting first-order optimality conditions with inequality constraints, including some remarks on numerical aspects. Furthermore, general initialization procedures are provided in order to extend the applicability of the unified flash to a more general setting (Section 3.2). In Section 4 a binary mixture of H2O–CO2 is modeled employing the Peng–Robinson EoS and an extension into the supercritical area is provided (Sections 4.1 and 4.2). Simulation results for wide ranges of pressure and temperature are presented along with comparisons to results obtained with the open-source package Thermo [14]. In Sections 4.3 to 4.5, examples for the unified flash procedure for specified p-T, p-h and h-v are presented and consistency of the framework is demonstrated. In a final example, the applicability of the unified isenthalpic flash is shown for a multicomponent mixture in Section 5.

2. State function based approach to the unified flash

The second law of thermodynamics states that a closed system approaches a state of maximum entropy at equilibrium, and any spontaneous process occurs so that the change in entropy s is non-negative [15], that is,

$$\delta \mathrm{s} > 0, \tag{2.1}$$

where δ denotes the inexact differential assuming spontaneous, irreversible changes can occur. To compute the equilibrium state of a fluid, two properties are assumed to be given at equilibrium, in addition to the mole numbers. In applications, the state is usually fixed in terms of p-T, p-h, T-v or u-v, using the standard notation for pressure, temperature and (specific) enthalpy, internal energy and volume respectively. The state function based approach to flash calculations leads for each pair of given properties to a target function which needs to be minimized, based on the second law and the fundamental thermodynamic relation [4]. We demonstrate in this section that the unified formulation of the p-T flash can be extended to other flash specifications by combining the state-function based approach and the unified formulation.

It is shown that the generalization of the unified flash displays a common mathematical structure for various specifications of state functions other than p-T. The underlying idea is to exploit the relation between state functions to be minimized and the Gibbs energy g. This is a quantity of central importance, since the first-order conditions for g result in the equality of chemical potentials and equivalently fugacities, which in the unified setting encodes the phase stability [11]. Furthermore, since other state functions like h and v can be expressed through partial phase properties weighed with phase fractions, constraints on the respective state functions can be initially included. The emerging mathematical structure is discussed at the end.

2.1. Unified flash for specified p-T

Consider at first the equilibrium problem for fixed pressure and temperature, for which the unified approach has already been applied successfully and analyzed [10,11]. We use this subsection to summarize the concept of the unified flash and to introduce the required notation.

Assume a non-reactive fluid mixture of $n_c \in \mathbb{N}$ components without solids, and given values of $\bar{p}$ and $\bar{T}$ at equilibrium. The bar symbol $\bar{\cdot}$ is used to denote constant quantities. Since $\delta \mathrm{s} > 0$, the fundamental thermodynamic relation must be an inequality of form [15]

$$\delta u < T\delta \mathrm{s} - p\delta v. \tag{2.2}$$

With the definition of the Gibbs energy in differential form,

$$\delta g = \delta u + \delta(pv) - \delta(T\mathrm{s}), \tag{2.3}$$

and pressure and temperature constant, inserting (2.3) into (2.2) leads to

$$\delta g < 0. \tag{2.4}$$

Hence, for given $\bar{p}$ and $\bar{T}$, the state function to be minimized is the Gibbs energy g of the fluid.

For a fluid mixture in the fractional formulation using moles, and a fixed context of $n_p \in \mathbb{N}$ phases, we introduce

1. overall molar fractions $\bar{z}_i,\ i \in \{1,\dots,n_c\}$, assumed given and constant,
2. molar phase fractions $y_j,\ j \in \{1,\dots,n_p\}$, and
3. relative fractions for component i in phase j denoted by x_{ij}.

The principle of mass conservation requires

$$\bar{z}_i - \sum_j y_j x_{ij} = 0,\ i \in \{1,\dots,n_c\}, \tag{2.5}$$

and unity constraints of form

$$\begin{aligned} 1 - \sum_i \bar{z}_i &= 0, \\ 1 - \sum_j y_j &= 0, \\ 1 - \sum_i x_{ij} &= 0,\ j \in \{1,\dots,n_p\}. \end{aligned} \tag{2.6}$$

Due to Eq. (2.6), an arbitrary phase r can be designated as the reference phase and its molar fraction can be replaced by the expression

$$y_r = 1 - \sum_{j \neq r} y_j. \tag{2.7}$$

Furthermore, an arbitrary mass conservation Eq. (2.5) can also be eliminated. The eliminated equation can be recovered using Eq. (2.6).

Remark 2.1. Throughout the remainder of this work, $n_c, n_p \geq 2$ are assumed. If $n_p = 1$, the equilibrium problem is trivial and the composition of the single phase equals the given overall composition $\bar{z}_i$. In the singular case $n_c = 1$ the single mass constraint cannot be excluded and the singularity is reflected in the injectivity of the resulting system of algebraic equations. To compensate for this case, it is possible to introduce a pseudo-component into the system with a small fraction $\bar{z}_i$ e.g., of order 1e−5 or lower, altering the properties of the mixture minimally. Here the unified formulation is an approximation of this singularity. It is a single degree of freedom case in the thermodynamic sense, by the virtue of the Gibbs phase rule.

Using a fixed context of n_p phases, the fractions y_j are allowed to take the value 0 in the unified setting, indicating a phase has vanished. Since the x_{ij} lose their physical meaning if $y_j = 0$, we introduce the extended fraction χ_{ij}. Ben Gharbia et al. [11] show in their analysis of the unified formulation the following particular properties of the extended fractions at equilibrium:

- If $y_j = 0$, then $0 \leq 1 - \sum_i \chi_{ij} \leq 1$.
- If $y_j \in (\,0, 1\,]$, then $\sum_i \chi_{ij} = 1$ and $\chi_{ij} = x_{ij},\ \forall i \in \{1, \dots, n_c\}$.
- The relation between x_{ij} and χ_{ij}, independent of the value of y_j, is given by re-normalization

$$x_{ij} = \frac{\chi_{ij}}{\sum_k \chi_{kj}}. \tag{2.8}$$

The introduction of extended fractions plays an important role in the unified formulation. They allow a choice of persistent variables. They also enable an evaluation of thermodynamic properties of vanished phases, i.e. the value of the state function to be minimized. This is required for a fluid mixture with a fixed context of n_p phases.

With above definitions, we can write the vector of persistent variables as

$$\mathbf{x} := \left[\dots, y_{j\neq r}, \dots, \chi_{11}, \dots, \chi_{n_c n_p}\right]^\top, \tag{2.9}$$

which is a total of $n_p - 1 + n_p n_c$ unknowns. By introducing the n-dimensional standard simplex

$$C_n = \left\{ x \in \mathbb{R}^n \;\middle|\; \sum_{k=1}^{n} x_k \leq 1 \text{ and } x_k \geq 0\ \forall k \right\}, \tag{2.10}$$

with $n \in \mathbb{N}$, we can write the domain of definition as

$$\Omega_{pT} = C_{n_p - 1} \times \underbrace{C_{n_c} \times \dots \times C_{n_c}}_{n_p}. \tag{2.11}$$

Finally, we introduce

$$\tilde{\mathbf{x}} = \left[\mathbf{x}, \{\bar{p}, \bar{T}\}\right], \tag{2.12}$$

which represents the generic argument for a thermodynamic quantity. The terms in curly brackets denote parameters. Following the Gibbs phase rule and assumptions made in Remark 2.1, we are allowed to express any state function in terms of $\tilde{\mathbf{x}}$.

With the introduced and fixed context of n_p phases and n_c components, the state function to be minimized (2.4) is the extended Gibbs energy of the fluid

$$g = \sum_j y_j g_j, \tag{2.13}$$

where g is represented using phase-related partial quantities g_j. We refer to it as *extended*, since g_j is included independent of whether y_j is zero or not. Furthermore, since Eq. (2.8) allows the representation $x_{ij} = x_{ij}(\tilde{\mathbf{x}})$ we can rewrite the target function as

$$g(\tilde{\mathbf{x}}) = \sum_j y_j g_j(\tilde{\mathbf{x}}). \tag{2.14}$$

Since y_j may take the value 0, we must require

$$y_j \geq 0,\ j \in \{1, \dots, n_p\} \tag{2.15}$$

explicitly. These inequality constraints ensure that a phase is either present ($y_j \in (\,0, 1\,]$) or absent ($y_j = 0$), and that $\mathbf{x} \in \Omega_{pT}$. The bound from above by 1 is implicitly included by the bound for the reference phase fraction (2.7). With Eqs. (2.5), (2.14) and (2.15), the equilibrium problem reads finally as:

Find $\mathbf{x}^\star \in \Omega_{pT}$ such that:

$$\mathbf{x}^\star = \underset{\mathbf{x}\in\Omega_{pT}}{\arg\min}\ g(\tilde{\mathbf{x}}), \tag{2.16}$$

$$\text{with:}\quad \bar{z}_i - \sum_j y_j \chi_{ij} = 0,\ i \in \{2, \dots, n_c\},$$

$$y_j \geq 0,\ j \in \{1, \dots, n_p\},$$

where the mass constraint for component 1 is eliminated following the comments on Eqs. (2.5) and (2.6). Recall that $\tilde{\mathbf{x}}$ depends on $\mathbf{x}$ and p, T are fixed in this case (2.12).

To solve Problem (2.16), we can use the Lagrange multiplier technique. The first order conditions for the extended Gibbs energy (2.14) lead to the equality of chemical potentials and equivalently equality of fugacities. This leads to infinitely many solutions if any y_j is zero. Hence we restrict ourselves to the case where the equality of fugacities also holds for phases that vanish. This choice corresponds to the unique, physical solution [11]. By doing so, we obtain

$$\begin{bmatrix} \Lambda(\tilde{\mathbf{x}}) \\ \Gamma(\mathbf{x}) \odot \lambda(\mathbf{x}) \end{bmatrix} = 0, \qquad \Gamma(\mathbf{x}),\ \lambda(\mathbf{x}) \geq 0, \tag{2.17}$$

where

$$\Lambda(\tilde{\mathbf{x}}) = \begin{bmatrix} \vdots \\ \left(\chi_{ij}\ \varphi_{ij}(\tilde{\mathbf{x}}) - \chi_{ir}\ \varphi_{ir}(\tilde{\mathbf{x}})\right)_{j\neq r} \\ \vdots \\ \left(\bar{z}_i - \sum_j y_j \chi_{ij}\right)_{i\geq 2} \\ \vdots \end{bmatrix}, \tag{2.18a}$$

$$\Gamma(\mathbf{x}) = \begin{bmatrix} y_1 \\ \vdots \\ y_{n_p} \end{bmatrix}, \tag{2.18b}$$

$$\lambda(\mathbf{x}) = \begin{bmatrix} 1 - \sum_i \chi_{i1} \\ \vdots \\ 1 - \sum_i \chi_{in_p} \end{bmatrix}, \tag{2.18c}$$

with $\odot$ denoting the component-wise Hadamard product and φ_{ij} the fugacity coefficient of component i in phase j. The isofugacity constraints in Eq. (2.18a) are formulated relative to the reference phase r. We refer the reader to any textbook on thermodynamics for their derivation [15]. Note that only Λ depends on $\tilde{\mathbf{x}}$, whereas Γ and λ depend solely on the fractional unknowns $\mathbf{x}$.

The steps required to arrive at Eqs. (2.17) and (2.18) starting from Eq. (2.16) are substantial. We refer to the remarkable results provided by Ben Gharbia et al. [11] and summarize the essential aspects in the following.

The equality of fugacities, complemented by the product of Eqs. (2.18b) and (2.18c) being zero, is proven to include the tangent-plane criterion. They capture the essential challenge of phase stability and are the reason why the unified formulation requires no stability checks. If the constraint $y_j = 0$ is active, phase j disappeared and its partial Gibbs energy g_j is cancelled by the zero weight (2.14). There is no need to change the set of variables (2.9) or Problem (2.16) as a whole. The feasibility of y_j and χ_{ij} is ensured by Eqs. (2.5) and (2.15), binding the fractional unknowns to the interval $[0, 1]$.

In total, System (2.17) contains $n_p - 1 + n_p n_c$ equations. It is consistent with the number of unknowns in $\mathbf{x}$ and well-posed with sufficient assumptions on g. It is non-smooth though, due to the complementarity conditions. The graph of (2.17) displays kinks at the border where a phase disappears or becomes saturated.

Problem (2.16) is general to the point where mathematical expressions are required for g_j and φ_{ij}, leading to mathematical properties of the target functional (2.14). As to the assumptions on g and consequentially φ_{ij}, their regularity and convexity depend on the thermodynamic model, which are critical for the well-posedness of the problem. We refer to [11,16] for discussions on various equations of state and heuristic laws.

2.2. Extended flash specifications

Section 2.1 introduced the equilibrium problem for given pressure and temperature, enabling a unified treatment of phase stability and

phase split calculations. The main question of the current work is how to use the unified approach if temperature or pressure or both are unknown at equilibrium. Since the presented p-T formulation relies on the Gibbs energy and consequently on the equality of fugacities to encode the tangent-plane criterion, the aim is to utilize that result and allow p or T to vary.

Here we show that System (2.17) can be extended in a direct manner to include state constraints for volume, enthalpy or internal energy if p or T are not specified initially. These extensions are shown to be thermodynamically consistent with the optimization approach for various flash types. They allow not only a unification of the phase stability and split calculations, but also a generalization in terms of state specifications for the fluid. The flash specifications treated here, p-h, T-v, u-v and h-v, display a common mathematical structure in the first-order conditions and allow a flexible switching between different flash types for different applications.

2.2.1. Isenthalpic constraint

Under narrow-boiling conditions, it is of interest to consider the equilibrium problem with a given enthalpy value $\bar{h}$ instead of temperature. Furthermore, for flow and transport problems it is natural to formulate an energy balance in terms of enthalpy and allow temperature to vary. In both cases, T becomes an additional unknown and $\tilde{\mathbf{x}}$ and the domain of definition must be modified such that

$$\tilde{\mathbf{x}} = [\mathbf{x}, T, \{\bar{p}\}], \tag{2.19a}$$

$$\Omega_{ph} = \Omega_{pT} \times (0, \infty). \tag{2.19b}$$

We show here how to expand the p-T flash System (2.17) by introducing an enthalpy constraint for given $\bar{h}$ and the definition of the (extended) fluid enthalpy

$$h = h(\tilde{\mathbf{x}}) = \sum_j y_j h_j(\tilde{\mathbf{x}}), \tag{2.20}$$

so that it is consistent with the state function based approach using maximization of entropy s.

For given $\bar{p}, \bar{h}$ and $\bar{z}_i$ the state function to be minimized is $-\mathrm{s}$ [4]. To combine this with the unified approach for phase split and stability introduced in Section 2.1, we use the definition of the Gibbs energy

$$g = u + pv - T\mathrm{s} = h - T\mathrm{s} = \bar{h} - T\mathrm{s}, \tag{2.21}$$

where we also included the target value for enthalpy $\bar{h}$ for the last equality. The state function to be minimized is replaced by

$$-\mathrm{s} = \frac{1}{T}(g - \bar{h}). \tag{2.22}$$

Since T is now a variable and a relation to the Gibbs energy g is established, we can perform the same steps leading to System (2.17), up to a multiplicative factor $1/T$ which can be eliminated. The difference is now that the first-order optimality conditions additionally demand the derivative with respect to T to be zero:

$$\frac{\partial}{\partial T}\left(\frac{1}{T}\left(g - \bar{h}\right)\right) = \frac{\partial}{\partial T}\left(\frac{g}{T}\right) + \frac{\bar{h}}{T^2} = 0. \tag{2.23}$$

Using the Gibbs–Helmholtz relation

$$\frac{\partial}{\partial T}\left(\frac{g}{T}\right) = -\frac{h}{T^2}, \tag{2.24}$$

Eq. (2.23) can be rewritten as

$$\frac{1}{T^2}\left(\bar{h} - h\right) = 0, \tag{2.25}$$

which by definition of the mixture enthalpy (2.20) and elimination of the multiplicative factor $1/T^2$ is equivalent to

$$\bar{h} - \sum_j y_j h_j(\tilde{\mathbf{x}}) = 0. \tag{2.26}$$

Given the above equivalence, the unified isenthalpic flash can be seen as a direct extension of its isothermal counterpart for the case when temperature is not fixed. The enthalpy "constraint" though, is *not* a constraint in the optimization sense, but a first-order condition resulting from using the thermodynamically consistent state function to be minimized. That is, the p-h flash in the unified setting is thermodynamically consistent.

An expansion of System (2.17) with an additional equation

$$Y_{ph}(\tilde{\mathbf{x}}) = \bar{h} - \sum_j y_j h_j(\tilde{\mathbf{x}}) = 0 \tag{2.27}$$

represents the isenthalpic flash in the unified setting, which exploits the inclusion of phase stability checks as introduced by Ben Gharbia et al. [11] for the isothermal flash. This is achieved by introducing the proper state function to be minimized (2.22) and its relation to the Gibbs energy, hence including implicitly the tangent-plane criterion [11, theorem 3.5].

2.2.2. Isochoric constraint

The idea introduced and applied so far in Section 2.2 can be adopted analogously to flash specifications where the pressure p is unknown at equilibrium. If p is unknown, we assume that the volume of the mixture $\bar{v}$, as its conjugated thermodynamic property, is given. This leads us to the isochoric flash, where $\bar{T}, \bar{v}$ and $\bar{z}_i$ are assumed to be given.

Under above specifications of the thermodynamic state, the second law and equilibrium conditions lead to the Helmholtz energy a as the state function to be minimized [15]. Using its definition and Eq. (2.21), the target function can be rewritten as

$$a = u - T\mathrm{s} = g - p\bar{v}, \tag{2.28}$$

which establishes a relation to the Gibbs energy g.

Again, following the steps from Section 2.1 we arrive at System (2.17) and need now to include the derivative with respect to p which ought to be zero. Since

$$\left(\frac{\partial g}{\partial p}\right)_{T \text{ fixed}} = v, \tag{2.29}$$

the extended optimality conditions include

$$\frac{\partial}{\partial p}(g - p\bar{v}) = -(\bar{v} - v) = 0. \tag{2.30}$$

For a mixture with multiple phases, the meaning of a mixture's volume v needs more elaboration. The notion of *volumetric* fractions s_j (saturations) must be introduced and its relation to the molar fraction y_j. The *saturated* molar density of a phase ρ_j is given in $[\mathrm{mol}\ /\ \mathrm{V}]$, where V is some volume measure related to the given value $\bar{v}$. If a single phase is saturated, the density of the mixture equals the phase density. If multiple phases are present, the mixture density is a sum of phase densities weighed by the fraction of space they occupy

$$\rho = \sum_j s_j \rho_j, \tag{2.31}$$

where s_j is allowed to take the value 0 in the unified setting. Note that the saturations s_j fulfill an analogous unity constraint (2.6), such that

$$s_r = 1 - \sum_{j \neq r} s_j. \tag{2.32}$$

can be eliminated as an unknown.

By the principle of mass conservation it holds that

$$y_j \rho = s_j \rho_j. \tag{2.33}$$

Eq. (2.33) trivially states that s_j is 0 or 1 if y_j is 0 or 1 and $\rho_j \neq 0$, $\forall j$. Using Eq. (2.31) and the definition of the specific volume as the reciprocal of density, we arrive at

$$v = \frac{1}{\sum_j s_j \rho_j}. \tag{2.34}$$

Isochoric flash specifications introduce additional $(n_p - 1) + 1$ unknowns, $s_{j \neq R}$ and p. Therefore we have now

$$\tilde{\mathbf{x}} = \left[\mathbf{x}, s, p, \{\bar{T}\}\right], \tag{2.35a}$$

$$\Omega_{Tv} = \Omega_{pT} \times C_{n_p-1} \times (0, \infty)\,, \tag{2.35b}$$

where $s = \left[\dots, s_{j\neq R}, \dots\right]^\top$ contains all independent saturation variables.

System (2.17) can be extended to include the first-order condition (2.30) and $n_p - 1$ relations of type (2.33), effectively closing the system. This leads to a new block of equations

$$Y_{Tv} = \begin{bmatrix} \bar{v} - v(\tilde{\mathbf{x}}) \\ \vdots \\ \left(y_j \rho(\tilde{\mathbf{x}}) - s_j \rho_j(\tilde{\mathbf{x}})\right)_{j\neq r} \\ \vdots \end{bmatrix} = 0, \tag{2.36}$$

where $v(\tilde{\mathbf{x}})$ and $\rho(\tilde{\mathbf{x}})$ are as in Eqs. (2.31) and (2.34).

2.2.3. Specification using u-v and h-v

In unsteady state applications like filling the container of fixed size with fluids, the fluid state is defined in terms of internal energy $\bar{u}$ and volume $\bar{v}$ at each time step [3]. Thus pressure *and* temperature are unknown at equilibrium. For what is known as the isoenergetic–isochoric flash, the state function to be minimized is also −s. Using Eq. (2.21) it can be rewritten as

$$-\mathrm{s} = \frac{1}{T}(g - \bar{u} - p\bar{v}). \tag{2.37}$$

The first-order optimality conditions now include the derivatives with respect to p and T. For p, we perform the same steps leading to Eqs. (2.29) and (2.30) and subsequently to (2.36). For T, using Eqs. (2.23) and (2.25) leads to

$$\frac{1}{T^2}(h - \bar{u} - p\bar{v}) = 0. \tag{2.38}$$

Inserting the definition of enthalpy

$$h = u + pv, \tag{2.39}$$

and using the volume constraint (2.30), yields

$$\frac{1}{T^2}(h - \bar{u} - p\bar{v}) = \frac{1}{T^2}(u - pv - \bar{u} - p\bar{v}) = -\frac{1}{T^2}(\bar{u} - u) = 0, \tag{2.40}$$

where the multiplicative factor $-1/T^2$ can be eliminated.

Combining System (2.17) with Eqs. (2.38) and (2.40), the unified u-v flash, like the previous flash types, can be represented using additional equations

$$Y_{uv} = \begin{bmatrix} \bar{u} - u(\tilde{\mathbf{x}}) \\ \bar{v} - v(\tilde{\mathbf{x}}) \\ \vdots \\ \left(y_j \rho(\tilde{\mathbf{x}}) - s_j \rho_j(\tilde{\mathbf{x}})\right)_{j\neq r} \\ \vdots \end{bmatrix} = 0, \tag{2.41}$$

with

$$\tilde{\mathbf{x}} = [\mathbf{x}, s, p, T]\,, \tag{2.42a}$$

$$\Omega_{uv} = \Omega_{pT} \times C_{n_p-1} \times (0, \infty)^2\,. \tag{2.42b}$$

The steps performed to derive the optimality conditions for the u-v flash can also be used for when $\bar{h}$ is specified instead of $\bar{u}$. There is an important difference though. The u-v-flash has the entire Ω_{uv} as its solution space (2.42b). The h-v flash on the other hand, where u is not fixed but implicitly given by

$$\bar{h} = u(\tilde{\mathbf{x}}) + p\bar{v}, \tag{2.43}$$

contains only a subset. A h-v-flash therefore is equivalent to an u-v-flash where the optimization is performed on the manifold defined by Eq. (2.43). The h-v-flash is a genuinely constrained problem in the optimization sense.

Table 1
Summary of relevant constraints in the unified setting for entropy-maximizing flash problems, their arguments and fixed state quantities.

	Y	$\tilde{\mathbf{x}}$
p-T	–	$[\mathbf{x}, \{\bar{p}, \bar{T}\}]$
p-h	$\begin{bmatrix} \bar{h} - \sum_j y_j h_j(\tilde{\mathbf{x}}) \end{bmatrix}$	$[\mathbf{x}, T, \{\bar{p}\}]$
T-v	$\begin{bmatrix} \bar{v} - v(\tilde{\mathbf{x}}) \\ \vdots \\ \left(y_j \rho(\tilde{\mathbf{x}}) - s_j \rho_j(\tilde{\mathbf{x}})\right)_{j\neq r} \\ \vdots \end{bmatrix}$	$[\mathbf{x}, s, p, \{\bar{T}\}]$
u-v	$\begin{bmatrix} \bar{u} - \sum_j y_j u_j(\tilde{\mathbf{x}}) \\ \bar{v} - v(\tilde{\mathbf{x}}) \\ \vdots \\ \left(y_j \rho(\tilde{\mathbf{x}}) - s_j \rho_j(\tilde{\mathbf{x}})\right)_{j\neq r} \\ \vdots \end{bmatrix}$	$[\mathbf{x}, s, p, T]$
h-v	$\begin{bmatrix} \bar{h} - \sum_j y_j h_j(\tilde{\mathbf{x}}) \\ \bar{v} - v(\tilde{\mathbf{x}}) \\ \vdots \\ \left(y_j \rho(\tilde{\mathbf{x}}) - s_j \rho_j(\tilde{\mathbf{x}})\right)_{j\neq r} \\ \vdots \end{bmatrix}$	$[\mathbf{x}, s, p, T]$

2.3. Comments on general structure and other flash types

The formulations presented in Section 2.2 indicate that the unified flash displays a general, mathematical structure and allows for a sandbox-type approach to formulating a suitable equilibrium problem. What changes is a subset of equations, which constrain thermodynamic state functions to a given value. The general structure of the unified flash is hence given by

$$\begin{aligned} \begin{bmatrix} \Lambda(\tilde{\mathbf{x}}) \\ Y(\tilde{\mathbf{x}}) \\ \Gamma(\mathbf{x}) \odot \lambda(\mathbf{x}) \end{bmatrix} &= 0, \\ \Gamma(\mathbf{x}),\ \lambda(\mathbf{x}) &\geq 0, \end{aligned} \tag{2.44}$$

with Y as in Eqs. (2.27), (2.36) and (2.41), and Λ, Γ, λ as in Eq. (2.18). The generic argument $\tilde{\mathbf{x}}$ contains p, s and/or T as independent state variables, depending on the flash specifications.

The reason why the first-order conditions of the considered problems display a common structure is the optimization approach based on the second law of thermodynamics. We have considered flash specifications where the entropy is maximal at equilibrium and exploited the relation between entropy and Gibbs energy, given by the Gibbs-Duhem equation

$$\mathrm{s} = -\frac{1}{T}(g - u - pv) = -\frac{1}{T}(g - h)\,. \tag{2.45}$$

Hence, the p-T, p-h, T-v, and u-v flash, as well as the h-v flash as a constrained u-v flash, fall into the class of entropy maximizing equilibrium problems. At their core they contain the equality of fugacities and conservation of mass represented by Λ, as well as the phase stability dynamics complemented by the condition $\Gamma \odot \lambda = 0$. The final definition of the fluid state at equilibrium is modeled with the block of equations $Y = 0$, which contains first-order conditions with respect to p and T as well as genuine constraints on thermodynamic quantities. A summary of relevant terms in Y and dependencies in $\tilde{\mathbf{x}}$ are given in Table 1.

Section 2.2.3 derived the h-v flash, where the additional constraint is not equivalent to the respective equilibrium criteria, which raises two questions. The first one is a question of well-posedness. The manifold (2.43), i.e. the value $\bar{h}$ must be within the feasible range of the thermodynamic model. Using arbitrary values for $\bar{h}$ and forcing $u(\tilde{\mathbf{x}})$ and p into regions where state functions display asymptotic behavior towards $\pm\infty$ will obviously cause any algorithm to fail. Once again, the unified

setting is as general as the chosen thermodynamic model allows and understanding the applied model plays an important role.

The second question concerns numerical aspects of optimization on manifolds, which poses a challenge of mathematical nature. Finding a descending direction which does not violate the constraint given by a manifold is a nontrivial task. Scenarios where the graph of Eq. (2.43) lies along a ridge of the state function to be minimized, where directional derivatives are of different magnitudes, are particularly sensitive to the choice of the descent direction. When formulating thermodynamic equilibrium criteria as first-order conditions of an optimization problem, it is crucial to understand which state functions are constrained and whether they place genuine constraints on the solution space.

Another class of flash problems not covered by above derivations constitutes systems with an a priori known entropy value $\bar{s}$ at equilibrium. Since entropy maximization would lead to trivial, necessary conditions, the problem must be reformulated as a minimization of total energy. Though the steps performed for obtaining the first-order optimality conditions leading to System (2.44) are general, the final expressions (2.18) are not necessarily the same. It is not clear how the unified setting can exploit the results presented in [11] in this case. While the procedure might be similar, it is out of the scope of this work and shall not be discussed further.

3. Numerical method

Section 2 presents the fluid phase equilibrium problem as an optimization problem with equality and inequality constraints, leading to non-smooth first-order conditions (2.44) and a generic argument $\tilde{\mathbf{x}}$.

To find the roots of System (2.44), Newton and Quasi-Newton methods are predominantly used. Smoothing techniques for the non-smooth complementarity conditions are also frequently applied. Recent discussions on solution strategies for this non-linear system are found in [17,18].

To our knowledge, there is no universally applicable method for arbitrary multiphase-multicomponent mixtures and flash types. Following trends in optimization [19], the interior-point methodology proposed by Vu et al. [17] provides an answer to many challenges involving non-linearities and constrained optimization, which appear when establishing the first-order conditions (2.44). Additionally, since convexity for the Gibbs energy g is in general not given, a more elaborate initial guess strategy is required if we aim for applying a Newton solver to find the roots. Otherwise the algorithm runs into the risk of descending to a local, non-physical minimum of the state function to be minimized, since the Newton method in the optimization sense is a gradient-descent method with full step-size.

In this section we present a numerical approach to solve the formulated equilibrium problems. It involves a non-parametric interior-point method (NPIPM) for the complementarity conditions, subsequently a standard Newton algorithm to find the roots of the resulting system of equations, and an Armijo line-search to provide a more robust step-size. The initialization procedures for different flash specifications, as well as the procedure for finding the roots of the resulting system are found as pseudo-algorithms in Appendix A.

3.1. The non-parametric interior-point method

The interior-point approach introduces a perturbed complementarity condition by allowing some scalar slack ν of form

$$\Gamma(\mathbf{x}) \odot \lambda(\mathbf{x}) - \nu \mathbf{1} = 0. \tag{3.1}$$

The choice of ν in the iterative sense must ensure a feasible update to $\mathbf{x}$. A desirable, iterative procedure ensures:

1. Starting from some admissible $\tilde{\mathbf{x}}$ and $\nu \geq 0$, as $\tilde{\mathbf{x}} \to \tilde{\mathbf{x}}^\star$, $\nu \searrow 0$ from above.
2. Non-negativity for $\Gamma(\mathbf{x})$ and $\lambda(\mathbf{x})$.
3. Recovery of the original System (2.44), including unperturbed complementarity conditions at convergence.

To achieve the properties stated above and to ensure an update to ν in a manner which reflects the state during iterations, a non-parametric approach is chosen. By turning ν into a variable of the problem, the system must be closed with an additional equation. Vu et al. [17] propose a slack equation of the form

$$\begin{aligned} f(\mathbf{x}, \nu) = &\frac{1}{2}\left(w \, \|\Gamma^-(\mathbf{x})\|^2 + \|\lambda^-(\mathbf{x})\|^2\right) \\ &+ \frac{u}{2n_p}\left(\langle \Gamma(\mathbf{x}), \, \lambda(\mathbf{x})\rangle^+\right)^2 + \nu^2 + \eta\nu, \end{aligned} \tag{3.2}$$

where $\|(\cdot)^-(\mathbf{x})\|^2$ ensures non-negativity of respective parts, $\langle\cdot,\cdot\rangle^+$ penalizes any violation of complementarity and a polynomial-type decline of ν is enforced. Given parameters u and η tune the penalty and the decline of ν. We included an additional parameter w to scale the penalty for cases where any phase fraction y_j violates the bounds $[0, 1]$. The augmented first-order conditions for the general flash read now as

$$\mathrm{F}(\tilde{\mathbf{x}}, \nu) = \begin{bmatrix} \Lambda(\tilde{\mathbf{x}}) \\ Y(\tilde{\mathbf{x}}) \\ \Gamma(\mathbf{x}) \odot \lambda(\mathbf{x}) - \nu \mathbf{1} \\ f(\mathbf{x}, \nu) \end{bmatrix} = 0. \tag{3.3}$$

Applying the Newton method requires an evaluation of the Jacobian matrix in every iteration, given by

$$\mathrm{DF} = \begin{bmatrix} \nabla_{\tilde{\mathbf{x}}} \Lambda(\tilde{\mathbf{x}}) & 0 \\ \nabla_{\tilde{\mathbf{x}}} Y(\tilde{\mathbf{x}}) & 0 \\ \nabla_{\tilde{\mathbf{x}}} (\Gamma(\mathbf{x}) \odot \lambda(\mathbf{x})) & \mathbf{1} \\ \nabla_{\tilde{\mathbf{x}}} f(\mathbf{x}, \nu) & \frac{\partial}{\partial \nu} f(\mathbf{x}, \nu) \end{bmatrix}. \tag{3.4}$$

With a pre-conditioning by multiplying the linearized, perturbed complementarity conditions with $\frac{u}{n_p}\langle \Gamma(\mathbf{x}), \, \lambda(\mathbf{x})\rangle$ and subtracting them from the last row in System (3.4), a proper decline of ν has been proven [17, prop. 3.1], hence guaranteeing convergence in a sufficiently small area around $\tilde{\mathbf{x}}^\star$. To increase the robustness, an Armijo line search in each iteration is included to obtain a step-size which reduces the residual of Eq. (3.3).

Remark 3.1 (*Conditioning*)**.** The algebraic system of nonlinear Eqs. (3.3) has two elements with negative impact on the Jacobian matrix (3.4) in terms of its condition number:

- The isofugacity constraints contained in Λ increase the overall condition number if the fugacity coefficients φ_{ij} become close to equal. This happens if the mixture approaches the supercritical state, where the liquid- and gas-like phases are not as distinguishable in terms of thermodynamic properties as in the subcritical region.
- The relaxed complementarity conditions and slack equation also impact the condition number negatively, if the same elements in Γ and λ both approach zero, leading to linearly dependent equations in the third and fourth row block of System (3.4). Furthermore, at the converged state the Jacobian DF reads roughly as

$$\begin{bmatrix} \nabla_{\tilde{\mathbf{x}}} \Lambda(\tilde{\mathbf{x}}^\star) & 0 \\ \nabla_{\tilde{\mathbf{x}}} Y(\tilde{\mathbf{x}}^\star) & 0 \\ \sim 0 & \mathbf{1} \\ \sim 0 & \frac{\partial}{\partial \nu} f(\tilde{\mathbf{x}}^\star, 0) \end{bmatrix},$$

  rendering System (3.3) inherently ill-conditioned. As the iterate approaches the solution $\tilde{\mathbf{x}}^\star$, the matrix DF loses its injectivity and becomes harder to invert, impacting the choice of the linear solver. In the authors' experience, direct solvers are robust when applied to such ill-conditioned systems and are the preferred choice in this work. While regularization techniques can be incorporated into f, experience showed that a sophisticated initial guess closer to $\tilde{\mathbf{x}}^\star$ outperforms attempts at modifying Eq. (3.2).

3.2. Initial guess strategy

System (3.3) is nonlinear, non-smooth, non-convex and displays possibly multiple roots, including roots in regions outside of the physical domain. In order to make the algorithm stable and reduce the number of iterations for a wide range of input data, we developed an initial guess strategy based on the classical successive-substitution approach. While we use the Rachford–Rice equations among others, purely heuristic initializations of values are available as well [3].

We assume a 2-phase mixture with only a gas and a liquid phase, and n_c components. An extension to multiple liquid phases is straightforward. The first goal is to compute a guess for fractional variables for given $\bar{p}, \bar{T}$ and $\bar{z}_i$. The gas fraction y is designated as the independent phase fraction. The initialization is started by computing a guess for the K-values using the Wilson-correlation,

$$K_i = \frac{\varphi_{iL}}{\varphi_{iG}} \approx \exp\left(5.37\,(1+\omega_i)\left(1-\frac{T_{c,i}}{\bar{T}}\right)\right)\frac{p_{c,i}}{\bar{p}},$$

with $\omega_i, T_{c,i}$ and $p_{c,i}$ denoting the component-specific acentric factor, critical temperature and pressure. The Rachford–Rice equation [20] in this case reads as

$$r(y) = \sum_i \frac{(K_i-1)\bar{z}_i}{1+y(K_i-1)} = 0. \tag{3.5}$$

Remark 3.2. For general multi-phase, multi-components mixtures, the Rachford–Rice equations must be solved numerically [8] using e.g., bisection or Brent's method. For the 2-phase, binary case, a direct inversion of Eq. (3.5) is readily obtainable as

$$y = \frac{\sum_{i\in\{1,2\}}(1-K_i)\bar{z}_i}{\sum_{i\in\{1,2\}}\left((K_i-1)\bar{z}_i(K_{k\neq i}-1)\right)}. \tag{3.6}$$

Solutions to Eq. (3.5) can yield nonphysical values $y \notin [0,1]$ and require a correction if so. Okuno et al. [8] present a potential for $r(y)$ with constant K-values which reads as

$$f(y) = \sum_i -\bar{z}_i \log\left(|1+y(K_i-1)|\right). \tag{3.7}$$

In combination with the requirement for non-negativity of phase compositions

$$\begin{aligned} 1+y(K_i-1)-\bar{z}_i &\geq 0\ \forall i,\\ 1+y(K_i-1)-K_i\bar{z}_i &\geq 0\ \forall i, \end{aligned} \tag{3.8}$$

a test of feasibility of the gas phase can be performed by assuming $y=1$. If $f(1)<0$ and the conditions (3.8) hold, the mixture is indeed gas-saturated and y is set to 1. If on the other hand $f(1)>0$, the mixture is liquid-saturated and y is set to 0.

Additional, stricter corrections are performed using the notion of the negative flash [21]. By computing the two innermost poles of Eq. (3.5),

$$\begin{aligned} \beta_1 &= \frac{1}{(1-\max\{K_i\})},\\ \beta_2 &= \frac{1}{(1-\min\{K_i\})}, \end{aligned} \tag{3.9}$$

and asserting that $\beta_1 < y < \beta_2$, y can be set to 0 if it is negative, or 1 if it is greater than 1.

Using the computed y, an initial guess for all χ_{ij} can be calculated via

$$\begin{aligned} \chi_{iL} &= \frac{\bar{z}_i}{1+y(K_i-1)},\\ \chi_{iG} &= \chi_{iL}K_i. \end{aligned} \tag{3.10}$$

The above steps can be repeated iteratively by recomputing the K-values after each iteration.

Remark 3.3. Note that this is essentially the successive-substitution approach to solving the equilibrium problem [7,8,22]. The difference is though, that the notion of extended phases (introduced in Section 4) is used here to recompute fugacity coefficients even for vanished phases. That is, no phase stability checks are performed for this initialization, compared to the classical successive-substitution approach.

We use a few iterations of this extended successive-substitution method and start with Newton iterations for System (3.3) subsequently, aiming for the minimum of the original state function to be minimized. The advantage gained by doing so is that we have obtained a guess closer to the solution and can in the end exploit the almost quadratic convergence provided by Newton's method.

If the temperature T is unknown and instead the enthalpy $\bar{h}$ is given, we guess the temperature and the fractions in an alternating manner. A first temperature value is obtained using the pseudo-critical quantity

$$T \approx \sum_i \bar{z}_i T_{c,i},$$

where $T_{c,i}$ is the critical temperature of present components. A first guess for fractions is obtained by solving the Rachford–Rice equation as shown above. Using a normalized enthalpy constraint

$$h_d = \frac{1}{\bar{h}}(h-\bar{h}) = 0, \tag{3.11}$$

the temperature can be updated using Newton iterations

$$\mathrm{d}T = \left(\frac{\partial}{\partial T}h_d\right)^{-1} h_d, \tag{3.12}$$

with fixed y and χ_{ij} to evaluate h, the enthalpy of the mixture (2.20).

Remark 3.4. As suggested by Zhu and Okuno [1], it is favorable to normalize *all* state constraints given in $\mathcal{Y}$ in Table 1 through division by the specified value. I.e., the step performed in (3.11) should be performed whenever a $\bar{h}, \bar{u}$ or $\bar{v}$ is given. This improves the conditioning and leads to less stiff systems.

After the temperature is updated, fractions are recomputed using Eqs. (3.6) and (3.10). Special care must be taken though when decoupling the iterative temperature update (3.12), and solving the Rachford–Rice equations for fixed T. This can easily lead to an unreasonable value for $\mathrm{d}T$ and consequently to a nonphysical, local minimum of System (3.3). To prevent the temperature update from shooting out into undesired regions, the value obtained by Eq. (3.12) can be chopped if it becomes unreasonably large. Additionally, a scaled step-size of

$$1-\frac{|\mathrm{d}T|}{T},$$

can be applied to the temperature update. Together with a frequently repeated update to fractions, a more robust initialization for the isenthalpic flash is obtained.

The idea behind the temperature initialization can be extended to an isochoric flash procedure where p, T and s are unknown. Starting from a pseudo-critical approximation for pressure and temperature [3], the initial values are refined using alternating updates for fractions and the additional unknowns. Fractions are again updated using the Rachford–Rice equation. The unknowns p, T and s are updated by solving the state constraints given by Eq. (2.41). Note that the update (3.12) is equivalent to solving Eq. (2.27) for temperature only. This analogy is motivated by the unified approach to state constraints. A flowchart for the complete numerical strategy is given in Fig. 1.

As previously mentioned, special care must be taken when decoupling the phase compositions calculation from the state constraints in $\mathcal{Y}$. If p or T are unknown, the ratio of the numerical parameters N_1, N_2 and N_3 (see Fig. 1) is critical due to the decoupling of molar fractions and state constraints given by $\mathcal{Y}$. The quantities h and v are sensitive to changes in p and T around phase borders, or in the liquid region where h varies strongly with T. This situation is aggravated by letting p and T vary simultaneously. For liquid-like states, the enthalpy changes minimally with a change in p due to $h = u + pv$ with v usually very small. If left unchecked, this relation causes oscillatory updates to p and T. Several corrective steps are required to obtain a reasonable initial

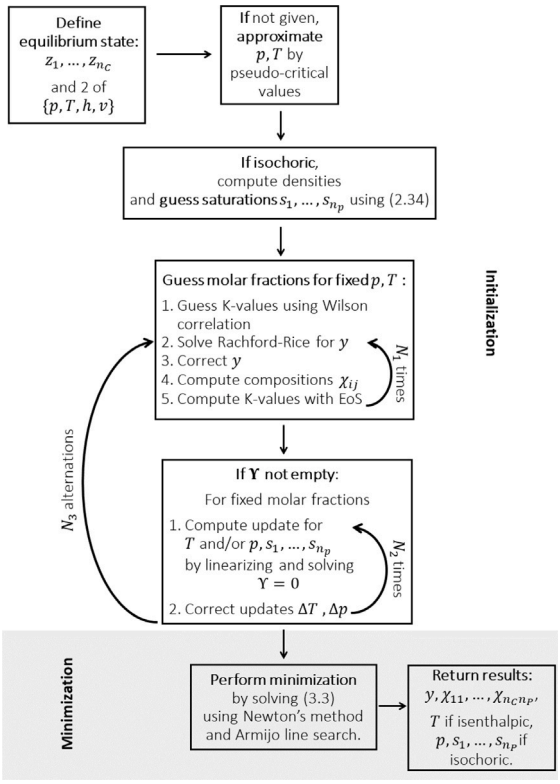

Fig. 1. A flowchart for the numerical approach including initialization. Note that the numbers $N_i, i \in \{1, 2, 3\}$, are assumed given and important for the robustness of the initial guess.

guess. For mixtures with a positive gas fraction and v exceeding $\bar{v}$, a negative pressure update is considered unstable. Additionally, due to a usually weak dependence of u on p and small v, initial guess strategies using specified $\bar{h}$ and $\bar{v}$ tend to neglect the compressing effect of p and instead decrease T. Therefore preference to positive pressure updates must be given to approach the solution from above in a stable manner. The corrective steps are summarized in Appendix A. Despite providing an overall good starting point, the initialization procedures presented here are rather expensive and require a finer tuning in terms in N_1, N_2 and N_3 in some challenging points.

4. Example: H2O–CO2 mixture using Peng–Robinson

This section presents the application of the unified formulation to a water and carbon dioxide mixture. To obtain expressions for fugacities and various state functions, the Peng–Robinson equation of state (PR EoS) is utilized as an example [12]. It is to this day the preferred choice in fluid reservoir engineering due to their precision and wide availability of required chemical data [23,24]. It is important to emphasize though, that this represents one example of how the unified procedure can be concretized in terms of expressions for thermodynamic quantities. More general flash procedures such as the isenthalpic one require additional thermodynamically consistent expressions for other state functions, and hence the EoS. Though the validity of the PR EoS under pure-liquid or near- and supercritical conditions is arguable when exact values for properties such as densities are required, it suffices to determine the multiphase regime, which is crucial for several subsurface flow applications.

At first we introduce the extension and labeling procedure for the sub-critical area, as proposed by Ben Gharbia et al. [11]. Then we propose a modified extension procedure in the supercritical region. Experimental data fitting the Widom-line for water [25] is used to distinguish between gas and liquid-like roots, enabling us to label the roots accordingly. Numerical tests for a H2O–CO2 mixture are performed subsequently, using the presented p-T, p-h and h-v flash in the unified setting. We demonstrate satisfying consistency of results for the p-T flash with values obtained from the package Thermo [14]. The unified p-h flash is applied along various isotherms to test its ability to recover the temperature correctly. The unified h-v flash is applied along an isotherm and isobar, again to test its ability to recover the pressure and temperature correctly. "Errors" in the sense presented here denote deviations between the results of the new procedures and the results from the p-T flash.

4.1. Phase labeling and extensions in the sub-critical region

The Peng–Robinson EoS models the p-v-T behavior of a fluid using the relation

$$p = \frac{R\,T}{v - b} - \frac{a}{v^2 + 2vb - b^2}, \tag{4.1}$$

where the cohesion and covolume a and b are obtained using experimental data and R is the universal, molar gas constant. By defining the respective dimensionless quantities A, B and the compressibility factor Z,

$$A = \frac{pa}{(RT)^2}, \quad B = \frac{pb}{RT}, \quad Z = \frac{pv}{RT}, \tag{4.2}$$

an algebraically equivalent cubic polynomial can be obtained:

$$Z^3 + (B-1)Z^2 + (A - 2B - 3B^3)Z + (B^2 + B^3 - AB) = 0 \tag{4.3}$$

At the critical point, A and B reach critical values A_c, B_c respectively. The compressibility factor Z is required to obtain EoS-specific expressions for φ_{ij}, h_j, g_j and ρ_j. Formulae for the Peng–Robinson EoS are given in Appendix B.

The value of A and B at each step of the solution procedure determines the number of real roots. Fig. 2 shows this number per A-B-pair. The critical point A_c, B_c is displayed as well as the critical line

$$B \geq \frac{B_c}{A_c}\, A. \tag{4.4}$$

In the area below the critical line and point,

$$W = \frac{1 - B - Z_1}{2} \tag{4.5}$$

is used as a substitute for the missing compressibility factor [11] in the regions with one real root Z_1 and two complex-conjugated roots (Fig. 2 on the left). The values are labeled according to their magnitude. The liquid phase is represented by the smaller and the gas phase by the larger value

$$\begin{aligned} W < Z_1 \quad &\rightarrow \quad Z_L = W,\ Z_G = Z_1, \\ W > Z_1 \quad &\rightarrow \quad Z_L = Z_1,\ Z_G = W. \end{aligned} \tag{4.6}$$

The narrow stripe below the critical line represents the gas region, bordering the subcritical three-root/two-phase region (Fig. 2 on the right). With increasing A, the two-phase region transitions into the liquid region, where again only one real root is available. At the critical point, Eq. (4.3) is known to display a single root with multiplicity 3. Furthermore, the borders between regions with one real root and regions with three real roots as well as the point $(0, 0)$, are known to display two real roots, where one has multiplicity 2. The two-root regions are lines and are not visible in Fig. 2 due to the refinement of the computations.

4.2. Labeling and extensions in the supercritical region

Fig. 2 on the left shows a shaded region above the critical line, indicating where the extended, liquid-like root violates the lower, physical bound given by the dimensionless covolume B. It also shows a

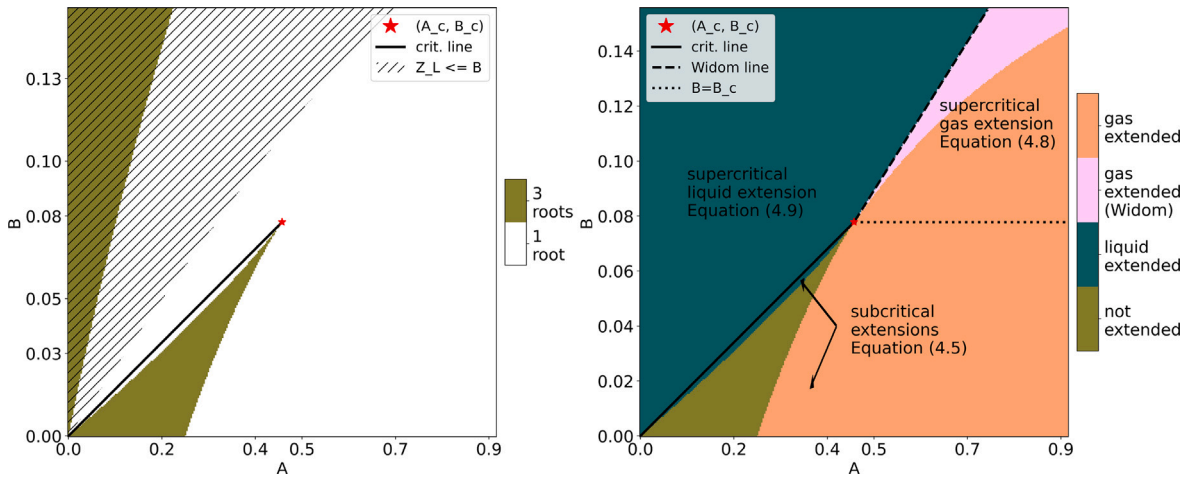

Fig. 2. (Left) Number of distinct real roots across a range of A-B points. The critical point and line are displayed, as well as regions where the physical bound B is violated by the extended, liquid root proposed in [11]. (Right) Usage of the extended roots for liquid and gas region. The Widom-line labeling results in a larger area where the extended root is assigned to the gas phase, compared to the labeling by size (4.6).

3-root region, where the smallest root is even negative. Those regions are not covered by the original extension proposed by Ben Gharbia et al. [11], as well as the area $B \geq B_c$. Here the smallest root of Eq. (4.3), as well as the original extension procedure fail to show physical results. Furthermore, Fig. 2 on the right shows an inconsistent labeling above the critical point when using the criteria (4.6) compared to Thermo. A larger area, bordered by the dotted and dashed line, is required to match the results.

To achieve this, the slope of the saturated liquid curve at the critical point is used to device a new labeling based on the Widom-line. Experimental data for water [25] was used and a linear fit of

$$B(A) = B_c + \frac{0.8}{2.95686087}(A - A_c), \; A \geq A_c, \tag{4.7}$$

is chosen to label the real and extended root. The slope of the saturated liquid curve at the critical point [11, Section 5.3] is given by 2.95686087. Below the Widom-line (4.7), the extended root is assigned to the gas phase, while the actual root is assigned to the liquid phase. Above it, the labeling is applied the other way.

On the right in Fig. 2 the effects of this choice are displayed by a larger region where the gas phase is labeled as the extended one. This causes the extended gas root to be slightly smaller than the real, liquid root in this particular area. The question whether this is reasonable or not is not answered here, since it presents an extended value, i.e. the gas-phase is not present and its thermodynamic properties have no meaning. The purpose of this extension is merely to stabilize the unified flash using the cubic PR EoS.

Remark 4.1. It should be noted that the exact Widom line can be characterized in the A-B space. The zeros of the second derivative of the departure enthalpy at constant pressure correspond to the theoretical Widom line [26, section 2]. Those points can be mapped onto the A-B space. This theoretical work is outside the scope of current research and will be addressed in the future.

Finally, to tackle the violation of the lower B-bound, an asymmetric extension W is proposed here. Below the Widom-line and above B_c, the extended gas-like root is computed by

$$W = \frac{1 - B - Z}{2} + B. \tag{4.8}$$

Eq. (4.8) is used as the extended, gas-like compressibility factor in the area denoted as "supercrit. gas extension". In the area denoted by "supercrit. liq. extension", the formula

$$W = Z - \frac{Z - B}{2}, \tag{4.9}$$

is used for the extended liquid-like root. To avoid discontinuities across the critical line, the Widom line and the line $B = B_c$, smoothing using a convex-combination of Eqs. (4.5), (4.8) and (4.9) is used in an small area around the lines separating the three areas with different extension procedures. Using a small number ϵ, the normal distances d to the lines is computed. After normalizing the distance by $l = d/\epsilon$, the extended root above the Widom-line (4.7) is given by

$$W = \begin{cases} (1 - B - Z)/2 + B & s = 0, \\ l\,((1 - B - Z)/2 + B) + (1 - l)\,(Z - (Z - B)/2) & 0 < l < 1, \\ Z - (Z - B)/2 & s = 1. \end{cases}$$

This is performed analogously above the critical line and the line $B = B_c$.

Remark 4.2. [11, theorem 6.3] derives a modified expression for fugacity coefficients using the PR EoS for the case when Eq. (4.5) is used to compute an extended compressibility factor. Additional terms are required to ensure smoothness of φ_{ij} across the phase boundaries and the critical line. These terms are neglected here and φ_{ij} is approximated using only the standard expression presented in Appendix B.

4.3. Isobaric–isothermal flash

Numerical tests were conducted for a H2O–CO2 mixture containing 1% CO2, i.e. $z_1 = 0.99$ and $z_2 = 0.01$. The flash calculations were performed for the ranges

$$p \in [1, 50] \text{ MPa},$$
$$T \in [450, 700] \text{ K},$$

which represent pressure and temperature conditions for a wide range of subsurface applications. A resolution of 80 points per axis was used and computations were performed for each p-T state. At most two phases are assumed to be present, a liquid and a gas phase, where the liquid one is set as the reference phase $r = 1$ and its fraction is eliminated by unity. The primary unknowns in this setting are the gas fraction y and four phase composition fraction χ_{ij}. The numerical procedure introduced in Section 3 was applied with solver parameters given in Table A.1 in the appendix.

Fig. 3 shows the resulting phase diagram (phase splits) given by this work and Thermo. A perfect match is observed in the subcritical region.

Fig. 4 shows the absolute error in y per point on the p-T diagram, where the results from Thermo are used as reference solutions. It also shows an increasing discrepancy between the solution provided by

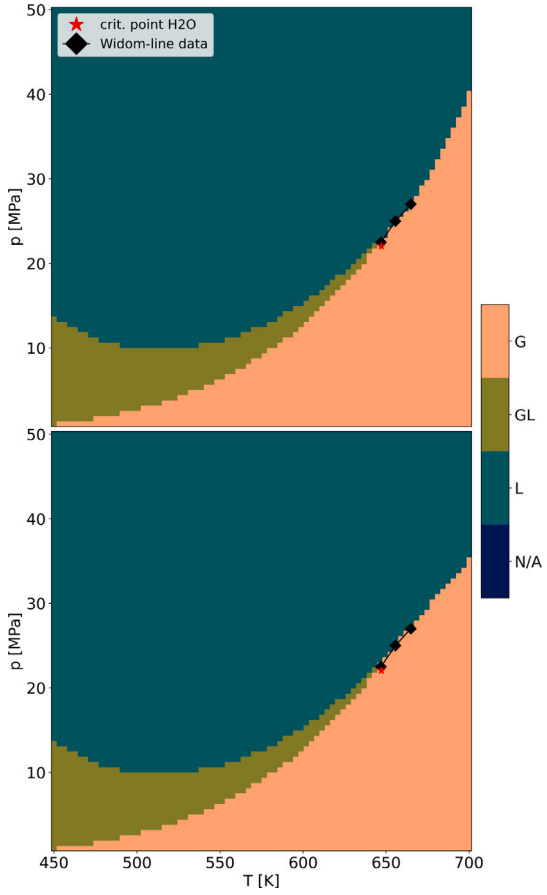

Fig. 3. (Top) Phase split results given by this work. The border between gas- and liquid-like regime in the supercritical area fits the approximated Widom-line [25]. (Bottom) Phase split according to Thermo. An increasing discrepancy between assigned gas- and liquid-like root is observed further into the supercritical area.

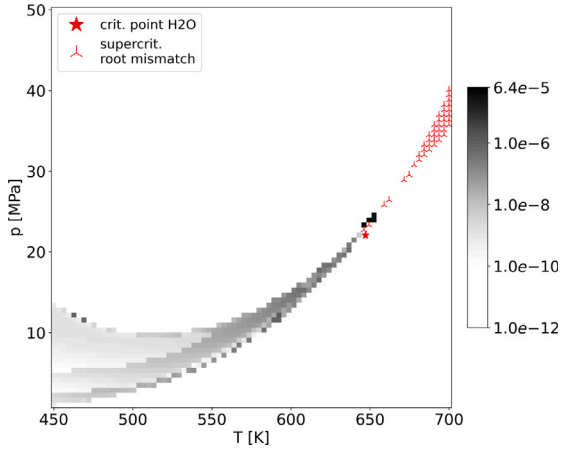

Fig. 4. Absolute error in gas fraction. A maximal error of 6.4e−5 is observed, compared to results computed by Thermo. Mismatching roots in the supercritical region are observed due to the approximation of the Widom-line. Here y takes the value 1 instead of 0, i.e. the gas phase is labeled as existing. Thermo on the other hand, labels the liquid phase as existing.

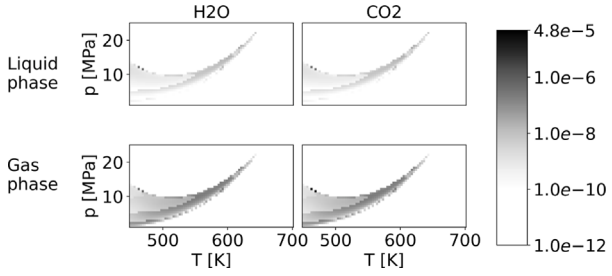

Fig. 5. Component fractions per phase, in the two-phase region between 1 and 25 MPa, and 450 and 640 K. A maximal error of 4.8e−5 is observed. The narrow stripe with increased errors indicates the region where water also starts evaporating. The wider region with small errors at low temperatures contains mostly CO2.

Thermo and by the unified flash further into the supercritical region. In points where y is indicated as zero by Thermo, this unified procedure indicates saturated gas. The labeling of phases in the supercritical regions introduced in Section 4.2 is performed based on a linearized Widom-line in the A-B space. The experimental data points are indicated in Fig. 3. A remedy to the observed discrepancy would be a better approximation of the Widom-line in the A-B space, which is clearly not linear further into the supercritical region. As pointed out by Maxim et al. [25], it is challenging to obtain respective data. It is straight-forward though to include them in the procedure presented in Section 4.2. Excluding the points of discrepancy, a satisfactory maximal error is observed, with the error generally increasing towards the critical point of water.

Fig. 5 shows the absolute error in phase compositions per component and phase in the two-phase region. As for y, the error in χ_{ij} displays a tendency to be larger towards the critical point. Errors outside the two-phase regions are trivially zero, since the respective phase compositions are consistent with the feed fractions due to mass conservation. A comparison of extended liquid phase compositions in the gas region, and vice versa extended gas compositions in the liquid region, could not be conducted, since respective data is not available from other flash procedures than the unified one.

Fig. 6 shows the number of iterations required when solving for the roots of Eq. (3.3) using the Newton method. The convergence criterion was reached in most points, with the exception of a few points mostly at the phase border in the supercritical region. At these points the number of maximal iterations was reached, where an oscillation of the residual around 1e−2 was observed. These oscillations are due to a phase being labeled as absent/extended or present, hence switching between different extended representations ((4.8), (4.9)) of the compressibility factor and the real root. Depending on where in the oscillation the algorithm stops, a saturated liquid- or gas-like root is returned. Convergence can be reached with an educated choice of the line-search parameters in individual cases.

As mentioned in Section 3.1, System (3.3) is inherently ill-conditioned. Fig. 7 shows the condition numbers after Newton convergence. The condition number is peaking along the saturated gas and liquid curves where the phase regime changes. Remark 3.1 explains the drastic increase in condition numbers.

The increasing unity gap for phase compositions can be observed in Fig. 8. The sum of fractions in gas and liquid phase respectively decreases from 1 and the unity gap becomes more apparent away from the two-phase region. Notice also that this cannot be observed in the supercritical area. All phase compositions are here close to the feed fraction since the K-values approach 1. The unity gap is directly related to the choice of extensions introduced in Eqs. (4.5), (4.8) and (4.9).

4.4. Isobaric–isenthalpic flash along isotherms

Consistency tests for the isenthalpic flash were performed using the isotherms

$$T \in [500, 550, 600, 640, 647.14, 650],$$

with 647.14 K being the critical temperature of water. Calculations were performed for pressure values in $[1, 23]$ MPa, with a resolution

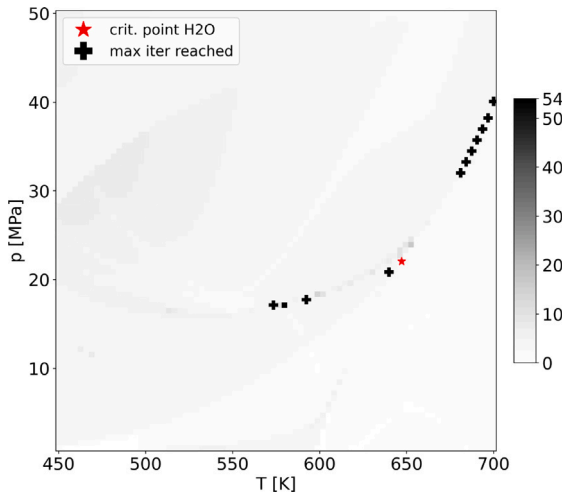

Fig. 6. Number of iterations per flash (excluding the initialization). At most 54 iterations were required. A few points did not converge after a given, maximal number of iterations. Modifying the solver parameters at individual points leads to convergence within the prescribed number of iterations. The average number of iterations, excluding the points where convergence was not reached, is ~ 3.

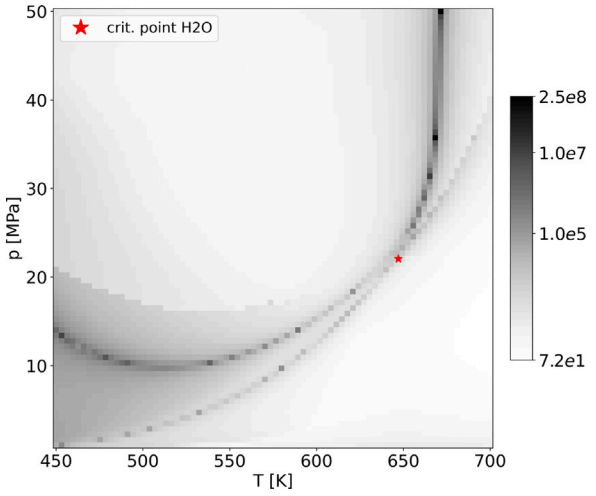

Fig. 7. Condition numbers of linearized System (3.3) after convergence. Phase borders display bad conditioning.

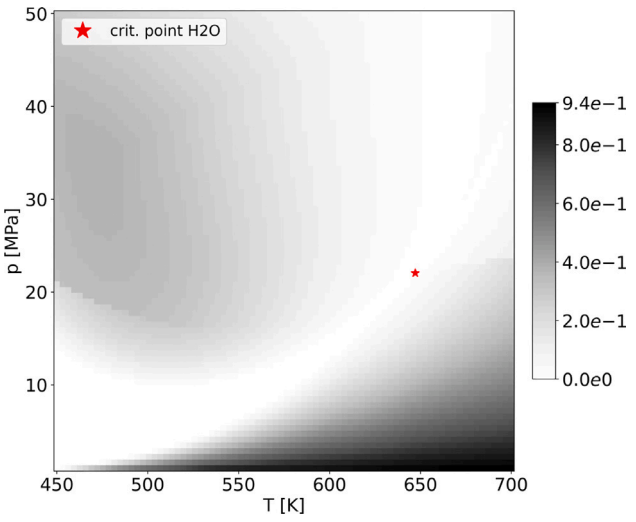

Fig. 8. Unity gap for gas composition in liquid region and liquid composition in gas region. In the two-phase region the unity gap is zero since there the component fractions coincide with the physical values.

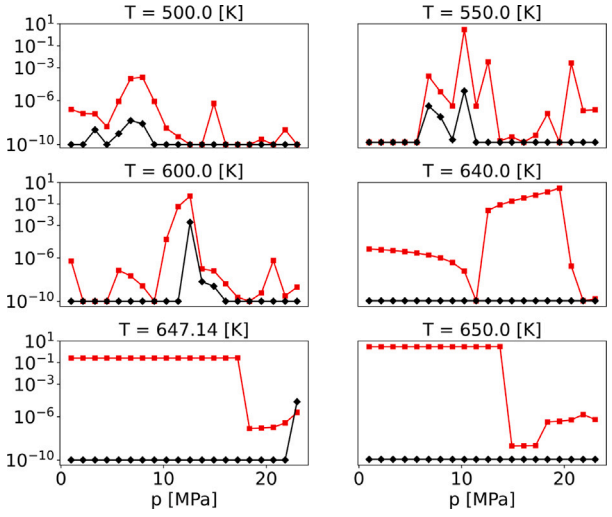

Fig. 9. Absolute errors per isotherm for T (red) and y (black). The maximal error in T is 0.547 K. The maximal error in y is 0.021. Errors below 1e−10 were capped for visualization purposes.

of 20 points. Resulting enthalpy values from a p-T flash were used to perform the unified p-h flash along each isotherm with refined pressure values, aiming for a recovery of the temperature. The solver settings are found in Table A.1.

Fig. 9 shows the absolute error in individual points and Fig. 10 the resulting L2-errors in T and y per isotherm. We can observe the isotherms crossing the two-phase region where the error in y displays a bump. It wanders wave-like to the right with increasing temperature, matching Fig. 3. Isotherms crossing the narrower two-phase region in Fig. 3 with temperatures ≥ 600 K display an increasing error peaking at the isotherm crossing the critical point. Nevertheless, the errors in T are well below 1 Kelvin in all points.

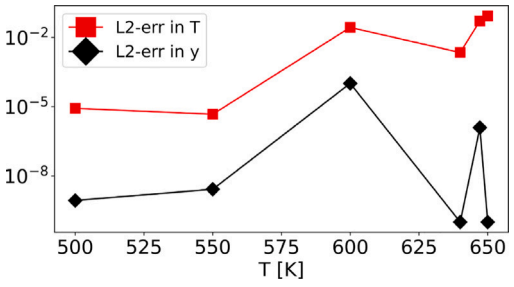

Fig. 10. The L2-error in T and y per isotherm. A generally larger error for isotherms crossing the narrower two-phase region is observed.

4.5. Isenthalpic–isochoric flash

Finally, to cover all extensions of the unified flash in terms of state definitions, calculations with specified enthalpy and volume are performed here and compared with results from the isothermal flash. The isobar $p = 15$ [MPa] with temperature ranging in $[575, 630]$ K and the isotherm $T = 575$ K with pressure ranging in $[5, 15]$ MPa were chosen to calculate volume and enthalpy. A resolution of 10 points was used per isoline. The isolines and ranges were chosen such that they traverse all three phase regions, liquid, two-phase and gas (Fig. 11).

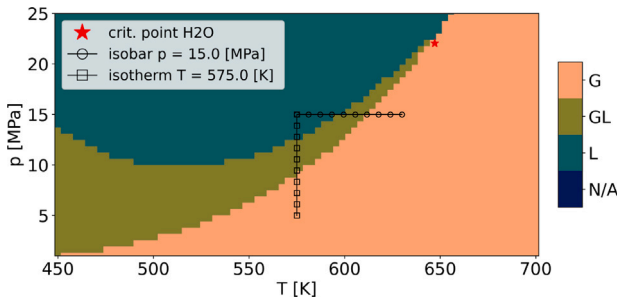

Fig. 11. Isolines and p-T points used to compute volume and enthalpy for the h-v flash.

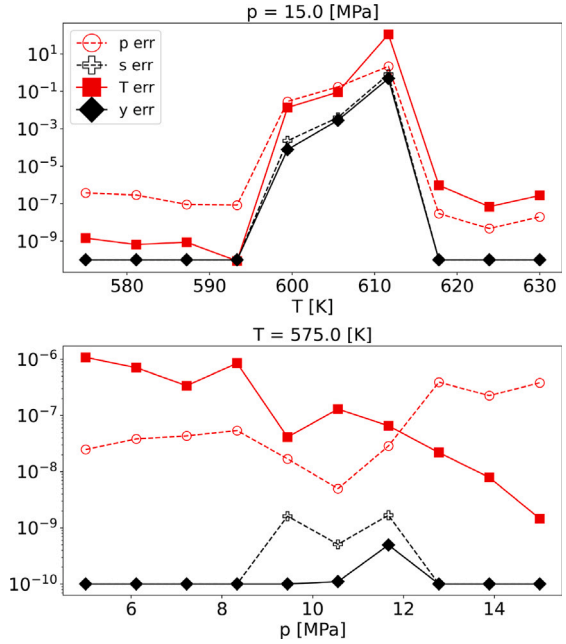

Fig. 12. Absolute errors along isolines $p = 15$ MPa and $T = 575$ K, for p, T, y and s.

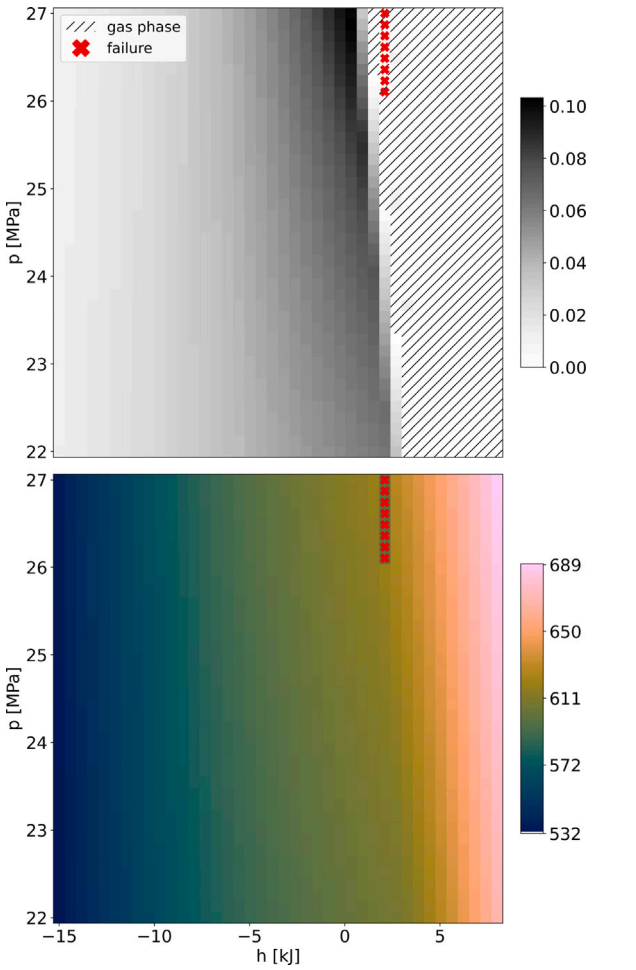

Fig. 13. (Top) Difference in gas fraction y compared to the results from Thermo. The points marked as failure indicate points where the algorithm did not succeed within the prescribed number of iterations. (Bottom) Resulting temperature in Kelvin. As expected in this case, no horizontal isotherms and hence no narrow-boiling is observed.

Analogously to Section 4.4, a recovery of pressure and temperature was aimed for.

Fig. 12 summarizes the results. The error profiles along the isolines display partially larger errors where they traverse through the two-phase region. Liquid water is only slightly compressible, resulting in close to vertical isochors in liquid-dominated regions. Furthermore, since enthalpy is a linear combination of internal energy and pressure-work (2.39), and internal energy varies strongly in T and weakly in p, increasing the temperature leads to a decrease in pressure for fixed volume and enthalpy. On top of the fluid volume being orders of magnitude smaller under liquid-like conditions, this leads to state specifications in terms of $\bar{h}$ and $\bar{v}$ being rather challenging. This is reflected respectively in large errors in the pressure recovery. To alleviate the circumstances, the Armijo line-search parameters are modified in order to obtain the results in Fig. 12. The maximal number of line search iterations was increased and the slope adjusted (see Table A.1). Even though it is straight-forward to perform h-v flash calculations in the unified setting, specifications in terms of $\bar{u}$ and $\bar{v}$ are more resilient [3,27].

5. Example: A multicomponent fluid mixture

For the second example we consider a more complex mixture by adding two components, hydrogen sulfide and nitrogen. As a motivation, this covers the most prominent chemical components found in geothermal fluids in the subsurface [28]. Søreide and Whitson [29] present a model where salt is treated as a pseudo-component to alter the boiling curve of other fluid components. Though this approach is compatible with the unified approach, since in essence it introduced the salinity only as a parameter in the cohesion term A in the PR EoS, we chose not to include it in order to compare with the results from Thermo.

We apply the isenthalpic flash in the unified setting to this vapor–liquid, four-component mixture with

$$\left[\bar{z}_{\mathrm{H2O}}, \bar{z}_{\mathrm{CO2}}, \bar{z}_{\mathrm{H2S}}, \bar{z}_{\mathrm{N2}}\right] = [0.8, 0.05, 0.1, 0.05].$$

Similar to Section 4, the range

$$p \in [22, 27] \text{ MPa},$$
$$h \in [-15, 8] \text{ kJ},$$

was chosen, with a resolution of 40 points per axis. While this example demonstrates the capability of the unified p-h flash to deal with multicomponent mixtures, it also shows its current limitations. Since our initialization is only concerned with at most two phases, we have to restrict the range of equilibrium states to cases where at most one liquid phase is observed. Computations in the supercritical area were not performed, since the labeling approach presented in Section 4.2 requires Widom-line data which is not available so far. For this challenging setting the solver parameters had to be adapted when

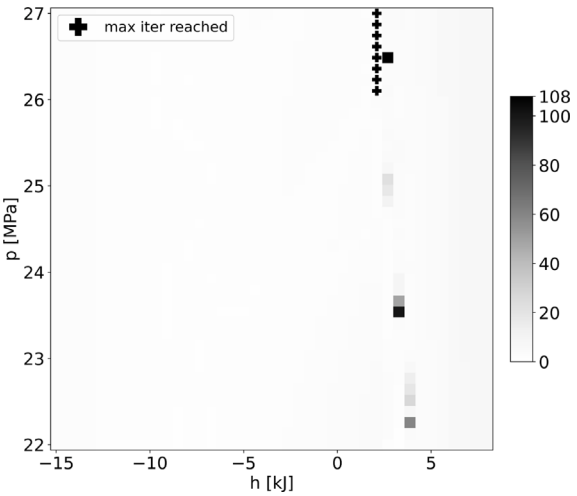

Fig. 14. Number of iterations per p-h flash (excluding the initialization). At most 108 iterations were required. The average number of iterations, excluding the points where convergence was not reached, is ∼3.3.

compared to Section 4.4 (see Table A.1). If the initialization was too far off and the flash did not converge, it was re-started with $(N_1, N_2, N_3) = (3, 3, 15)$. Additionally, the maximal number of line search iterations was increased to 70. The parameter adjustment was done only once.

Fig. 13 shows the results for the difference in y and the distribution of T. A phase split consistent with the results from Thermo was achieved, with a difference of up to 10% in y. This discrepancy may be attributed to a difference in the computation of the enthalpy, which consists of the ideal part and the EoS-specific departure function. This work used a set of coefficients to interpolate the ideal part [1,2,30]. They are found in Table B.3 in the appendix. Thermo on the other hand performs a numerical integration to obtain the ideal part.

Fig. 14 displays the number of iterations for this range of equilibrium configurations. For the 1600 combinations of p and h, 8 failed to converge with above solver settings. We attribute all failures to lack of a universally robust initialization procedure. Indeed, for the failed computations, a modification of the parameters N_1, N_2 and N_3 lead to initialization closer to the physical minimum. The initialization procedure can also be replaced by arguments based on the duality principle [31], where the solution of the dual problem provides all the information necessary to reconstruct all stable phases in a given thermodynamic state. It is possible to solve such problems numerically using the procedures given by Jungen et al. [32]. In spite of this, such approaches are outside the scope of the present study and are left for future investigation.

6. Conclusion

The unified flash procedure was shown to be capable of calculating the vapor–liquid equilibrium of mixtures for general state definitions and multiple components. Entropy-maximizing equilibrium calculations display a unified structure not only for handling the appearance and disappearance of phases but also for constraints on thermodynamic state functions. The presented procedures are able to consistently recover pressure and/or temperature for problems where they are unknown at equilibrium. This extends the field of applications for the unified flash to a wide range of problems.

The structure of Eq. (2.44) exposes the nature and the challenges of computing fluid phase equilibria, which can be divided into computing the equilibrium fractions, the correct phase split and finally constraints to state functions. It also shows that these three aspects can be modeled mathematically with a closed system of equations and unknowns.

The non-parametric interior-point method together with a sophisticated initial guess strategy, which approximates the phase split at equilibrium, was shown to be a reliable solution strategy for the general unified flash. Though further work on the initialization is required to increase its efficiency, i.e. to avoid the decoupling of volume and enthalpy from phase fractions.

The enhancement of the extension procedure for compressibility factors enables mixture models using the Peng–Robinson EoS for a wider range of pressure and temperature values, including the supercritical region. To better approximate the gas- and liquid-like regimes in the supercritical area, more experimental data is required to represent the phase border in the A-B space. Once available, the unified approach allows for a seamless integration of physical models and respective data.

Finally, an essential advantage of the unified approach and the extension and labeling of compressibility factors, is the elimination of phase stability tests. They are neither required for the initialization nor the minimization process. This advantage is reflected in efficient implementations, where the number of anticipated phases is fixed.

Nomenclature

p	pressure [Pa]
T	temperature [K]
v	specific molar volume [m^3 / mol]
h	specific molar enthalpy [J/mol]
u	specific molar internal energy [J/mol]
g	specific molar Gibbs energy [J/mol]
s	specific molar entropy [J/K mol]
φ	fugacity coefficient [–]
R	ideal molar gas constant [J/mol K]
z	overall molar component fraction [–]
y	molar phase fraction [–]
s	volumetric phase fraction (saturation) [–]
x	physical molar fraction of component [–]
χ	extended molar fraction of component [–]
ν	NPIPM slack variable
$\mathbf{x}$	vector of fractional unknowns
$\tilde{\mathbf{x}}$	generic argument for thd. quantities
$(W)\ Z$	(extended) compressibility factor
ω	acentric factor [–]
a	cohesion [Pa mol^2 / $m^{3\cdot2}$]
b	covolume [m^3 / mol]
A	non-dimensional cohesion [–]
B	non-dimensional covolume [–]
n_c	number of components
n_p	number of phases
i,k	component indices
j	phase index
r	index of reference phase
G,L	gas and liquid phase indices
c	index for critical values
$\bar{\cdot}$	given and constant value

CRediT authorship contribution statement

V. Lipovac: Conceptualization, Methodology, Software, Writing – original draft, Visualization. **O. Duran:** Conceptualization, Supervision, Methodology, Software, Validation, Writing – review & editing. **E. Keilegavlen:** Conceptualization, Supervision, Writing – review & editing. **F.A. Radu:** Conceptualization, Supervision, Writing – review & editing. **I. Berre:** Conceptualization, Supervision, Writing – review & editing, Project administration, Funding acquisition.

Declaration of competing interest

The authors declare that they have no known competing financial interests or personal relationships that could have appeared to influence the work reported in this paper.

Data availability

The data and source code for the results presented herein is available, and the plots can be reproduced using a Docker container available at: https://doi.org/10.5281/zenodo.8273367.

Acknowledgments

This project has received funding from the European Research Council (ERC) under the European Union's Horizon 2020 research and innovation program (grant agreement No 101002507).

Appendix A. Pseudo-algorithms

Initialization procedures are constructed by considering the guess for phase fractions and compositions, and the guess for pressure and/or temperature separately. For guessing the phase fractions and compositions, pressure and temperature are kept constant. For guessing p or T, the composition is kept constant. Feed fractions $\bar{z}_i$ are assumed given and constant at all times.

For two-phase mixture with arbitrary many components, an initial guess for the gas-fraction y and χ_{ij} at constant $\bar{p}$ and $\bar{T}$ is provided using the Rachford–Rice equations. Corrections to nonphysical phase fractions are performed using insight from the negative flash and a potential provided by Okuno et al. [8]. This procedure is used to provide initial fractions for the p-T flash.

Algorithm 1: p-T-based initialization of fractions

Require: $N_1, \bar{p}, \bar{T}, \bar{z}_i$
Ensure: $n_p = 2$
if K-value guess required (Wilson correlation) **then**
  $K_i \leftarrow \exp\left(5.37\left(1+\omega_i\right)\left(1-\frac{T_{c,i}}{\bar{T}}\right)\right)\frac{p_{c,i}}{\bar{p}}$
else
  $K_i \leftarrow \varphi_{iL}/\varphi_{iG}$ from EoS $\forall i$
end if
for $l = 1 \dots N_1$ **do**
  if $n_c == 2$ **then**
    $y \leftarrow \dfrac{\sum_i (1-K_i)\bar{z}_i}{\sum_i \left((K_i-1)\bar{z}_i \sum_{k\neq i}(K_k-1)\right)}$
  else
    $y \leftarrow$ solve Eq. (3.5) using Brent's method
  end if
  $y \leftarrow$ correction if nonphysical
  $\chi_{i,L} \leftarrow \bar{z}_i/(1+y(K_i-1)),\ \forall i$
  $\chi_{i,G} \leftarrow K_i \chi_{i,L},\ \forall i$
  $K_i \leftarrow \varphi_{iL}/\varphi_{iG}$ from EoS $\forall i$
end for
return $1-y, y, x_{ij}$

Algorithm 2: Correction of nonphysical gas fractions

Require: $y, \bar{z}_i, K_i$
Ensure: $n_p = 2$
$\beta_1, \beta_2 \leftarrow 1/(1-\max\{K_i\}), 1/(1-\min\{K_i\})$
$f \leftarrow \sum_i -\bar{z}_i \log\left(|1+(K_i-1)|\right)$
feasible $\leftarrow \beta_1 < y < \beta_2$
for $i = 1 \dots n_c$ **do**
  $\text{condition}_{1,i} \leftarrow 1+(K_i-1)-\bar{z}_i \geq 0$
  $\text{condition}_{2,i} \leftarrow 1+(K_i-1)-K_i\bar{z}_i \geq 0$
end for
if $(y<0 \vee y>1) \wedge f > 0$ **then**
  $y \leftarrow 0$
else if $(y<0 \vee y>1) \wedge f < 0$ $\wedge(\text{condition}_{1,i}\forall i) \wedge (\text{condition}_{2,i}\forall i)$ **then**
  $y \leftarrow 1$
end if
if feasible $\wedge\ y<0$ **then**
  $y \leftarrow 0$
else if feasible $\wedge\ y>1$ **then**
  $y \leftarrow 1$
end if
return y

For flash procedures with unknown temperature, a pseudo-critical temperature is computed at first, followed by an alternating update for fractions and temperature, each for fixed temperature and fractions respectively.

Algorithm 3: p-h flash initialization

Require: $N_1, N_2, N_3, \bar{p}, \bar{h}, \bar{z}_i$
$T \leftarrow \sum_i \bar{z}_i T_{c,i}$
$y, x_{ij} \leftarrow$ p-T-based initialization with $N=2$
for $l_1 = 1 \dots N_3$ **do**
  for $l_2 = 1 \dots N_2$ **do**
    $h \leftarrow$ from EoS
    $h_d \leftarrow (h-\bar{h})/\bar{h}$
    $\mathrm{d}T \leftarrow -h_d/\frac{\partial}{\partial T}h_d$
    $\mathrm{d}T \leftarrow 0.1T\ \text{sign}(\mathrm{d}T)$, if $|\mathrm{d}T| > T$
    $T \leftarrow T + (1-|\mathrm{d}T|/T)\mathrm{d}T$
  end for
  $y, \chi_{ij} \leftarrow$ p-T initialization, line 4 with N_1
end for
return $T, 1-y, y, x_{ij}$

If the pressure is an additional unknown in the flash, it is also initialized using a pseudo-critical approximation involving the given volume. The guess is subsequently refined using the state constraints on $\bar{h}$ and $\bar{v}$.

Algorithm 4: Pseudo-critical initialization of p and T

Require: $\bar{h}, \bar{v}, \bar{z}_i, T_{c,i}, v_{c,i}$
$T \leftarrow \sum_i \bar{z}_i T_{c,i}$
$v \leftarrow \sum_i \sum_k \bar{z}_i \bar{z}_k/8(v_{c,i}^{1/3}+v_{c,k}^{1/3})^3$
$r \leftarrow v/\bar{v}$
if $r > 1$ **then**
  $Z \leftarrow 0.2$, liquid-like root
  $T \leftarrow T/r^2$, temperature correction
else
  $Z \leftarrow 0.7$, gas-like root
end if
$p \leftarrow ZTR/\bar{v}$
$y, \chi_{ij} \leftarrow$ p-T-initialization with $N=3$
if $y < 1\text{e}-3$ **then**
  $p \leftarrow 0.7p$
end if
return p, T

Algorithm 5: Improved initial guess for p and T

Require: $N_1, N_2, N_3, \bar{h}, \bar{v}, \bar{z}_i$
$p, T \leftarrow$ pseudo-critical initialization
$y, \chi_{ij} \leftarrow$ p-T-based initialization, line 4 with N_1
for $l_1 = 1 \dots N_3$ **do**
  for $l_2 = 1 \dots N_2$ **do**
    $h_j, \rho_j \leftarrow$ from EoS $\forall j$
    $s \leftarrow$ solve using Eq. (2.33)
    $h, \rho, v \leftarrow$ using y, s, ρ_j, h_j
    $\mathrm{d}p, \mathrm{d}T, \mathrm{d}s \leftarrow$ solve Y_{hv} for p, T, s
    chop $\mathrm{d}T$ and $\mathrm{d}p$ if unreasonably large
    if $\neg(y > 1\text{e}-3 \wedge v > \bar{v} \wedge \mathrm{d}T < 0)$ **then**
      preference to compression with p
      $T \leftarrow T + (1-|\mathrm{d}T|/T)\mathrm{d}T$
    end if

Table A.1
Solver parameters used in Section 4.
The initialization algorithms were performed using N_1, N_2 and N_3 (see Fig. 1). The prescribed number of iterations for Newton's method and Armijo line search are N_N and N_A respectively. The convergence criterion is given by ϵ for the residual tolerance of Eq. (3.3). Symbols σ and τ denote the line search parameters and η, u and w the NPIPM parameters.

	p-T	p-h	h-v
N_1	3	3	2
N_2	–	1	2
N_3	–	5	7
N_N	150	150	150
N_A	50	30	150
ϵ	1e−8	1e−8	1e−8
σ	0.99	0.99	0.9
τ	0.4	0.4	0.4
η	0.5	0.5	0.5
u	1	1	1
w	10	1	10

if $\neg(y > 1\text{e}-3 \wedge v > \bar{v} \wedge \mathrm{d}p < 0)$ **then**
  only stable p-update
  $p \leftarrow p + (1 - |\mathrm{d}p|/p)\mathrm{d}p$
end if
if $v > \bar{v} \wedge y = 1$ **then**
  correction for gas-like mixtures
  $p \leftarrow (1 + |\mathrm{d}p|/p)p$
else if $h < \bar{h} \wedge y < 0.1$ **then**
  correction for liquid-like mixtures
  $p \leftarrow 1.1p$
end if
end for
$y, \chi_{ij} \leftarrow$ p-T-based initialization, line 4 with N_1
end for
$\rho_j \leftarrow$ from EoS $\forall j$
$s \leftarrow$ solve using Eq. (2.33)
return $p, T, 1-s, s, 1-y, y, \chi_{ij}$

After an initial guess is computed, Newton iterations including an Armijo line search are performed to find the root of Eq. (3.3). An initial estimate for the slack variable ν is provided using the fractions.

Algorithm 6: NPIPM with Armijo line-search

Require: $N_N, N_A, \epsilon, \bar{z}_i, u, \eta, \tau \in (0, 1/2), \sigma \in (0, 1)$
$(s, p, T,)y_j, \chi_{ij} \leftarrow$ from initialization
$\nu \leftarrow (\sum_j y_j(1 - \sum_i \chi_{ij}))/n_p$
$\tilde{\mathbf{x}} \leftarrow (s, p, T,)\ y_j, \chi_{ij}$ assemble solution vector
if $|\mathrm{F}(\tilde{\mathbf{x}})| \le \epsilon$ **then**
  return $\tilde{\mathbf{x}}$
else
  for $l = 1 \dots N_N$ **do**
    $\mathrm{d}\tilde{\mathbf{x}} \leftarrow \mathrm{DF}^{-1}(\tilde{\mathbf{x}})\mathrm{F}(\tilde{\mathbf{x}})$
    for $j = 1 \dots N_A$ **do**
      $\tilde{\sigma} \leftarrow \sigma^j$
      if $\frac{1}{2}\left|\mathrm{F}(\tilde{\mathbf{x}} + \sigma^j \mathrm{d}\tilde{\mathbf{x}})\right|^2/2 \le (1 - 2\tau\sigma^j)\frac{1}{2}|\mathrm{F}(\tilde{\mathbf{x}})|^2$ **then**
        break
      end if
    end for
    $\tilde{\mathbf{x}} \leftarrow \tilde{\mathbf{x}} + \tilde{\sigma}\mathrm{d}\tilde{\mathbf{x}}$
    if $|\mathrm{F}(\tilde{\mathbf{x}})| \le \epsilon$ **then**
      return $\tilde{\mathbf{x}}$
    end if
  end for
end if

Table B.1
Component parameters required for PR EoS.

Comp.	T_c [K]	p_c [Pa]	ω
H2O	647.14	22048320.0	0.344
CO2	304.2	7376460.0	0.2252
H2S	373.2	8 936 865	0.1
N2	126.2	3394387.5	0.04

Table B.2
Matrix of binary interaction parameters k_{ij}, taken from [14]. Note that $k_{H2O,N2}$ is zero, which is questionable. More reliable interaction coefficient values are available in e.g. [33].

	H2O	CO2	H2S	N2
H2O		0.0952	0.0394	0
CO2			0.0967	−0.0122
H2S				0.1652

Appendix B. Expressions for Peng–Robinson EoS

For mixtures with $i, k = 1 \dots n_c$ components, applying the Van-der-Waals mixing rule results in cohesion a_j and covolume b_j for phase j being of form

$$a_j = \sum_i \sum_k x_{ij} x_{kj} \hat{a}_{ik}, \quad b_j = \sum_i x_{ij} \hat{b}_i, \tag{B.1}$$

with component-specific terms

$$\hat{b}_i = B_c \frac{RT_{c,i}}{p_{c,i}}, \tag{B.2}$$

$$\hat{a}_{ik} = \sqrt{\hat{a}_i \hat{a}_k}(1 - k_{ij}), \tag{B.3}$$

$$\hat{a}_i = A_c \frac{R^2 T_{c,i}^2}{p_{c,i}} \alpha_i(T), \tag{B.4}$$

and non-dimensional quantities

$$A_j = \frac{pa_j}{(RT)^2}, \quad B_j = \frac{pb_j}{RT}, \tag{B.5}$$

$$\frac{\partial A_j}{\partial T} = \frac{1}{RT}\frac{\partial a_j}{\partial T} - \frac{2a_j p}{R^2 T^3}, \tag{B.6}$$

$$\frac{\partial A_j}{\partial x_{ij}} = 2\sum_k x_{ik} a_{ik}. \tag{B.7}$$

For the Peng–Robinson EoS it holds:

$$\sqrt{\alpha_i(T)} = 1 + \kappa(\omega_i)\left(1 - \sqrt{\frac{T}{T_{c,i}}}\right), \tag{B.8}$$

$$\kappa(\omega) = \begin{cases} 0.37464 + 1.54226\omega - 0.26992\omega^2 & \omega < 0.491, \\ 0.379642 + 1.48503\omega - 0.164423\omega^2 + 0.016666\omega^3 & \omega \ge 0.491, \end{cases} \tag{B.9}$$

$$A_c = \frac{1}{512}\left[-59 + 3\sqrt[3]{276231 - 19512\sqrt{2}} + 3\sqrt[3]{276231 + 19512\sqrt{2}}\right], \tag{B.10}$$

$$B_c = \frac{1}{32}\left[-1 + 3\sqrt[3]{16\sqrt{2} - 13} + 3\sqrt[3]{16\sqrt{2} + 13}\right]. \tag{B.11}$$

Values for critical pressure, temperature, the acentric factor ω and binary interaction coefficients k_{ik} are given in Tables B.1 and B.2. The corrective factor $\kappa(\omega)$ is given as in [1, appendix A-1]. The ideal molar gas constant is $R = 8.31446261815324$ [J/(K mol)].

After computing the (extended) roots Z_j of Eq. (4.3) and labeling them, partial phase properties can be evaluated. State functions and fugacity coefficients used in this work include:

$$\rho_j = \frac{1}{v} = \frac{p}{RTZ_j}, \tag{B.12}$$

Table B.3
Heat capacity coefficients at constant pressure with SI units [J/(mol K^i)] for $c_{p,k}$.

	H2O	CO2	H2S	N2
$c_{p,1}$	32.2	19.795	3.931	3.28
$c_{p,2}$	1.907e−3	7.343e−2	1.49e−3	0.593e−3
$c_{p,3}$	1.055e−5	−5.602e−5	−0.232e5	0.04e5
$c_{p,4}$	−3.596e−9	1.715e−8	–	–

$$g_j = \sum_i x_{ij} \log x_{ij} + g_j^{\text{dep}}, \tag{B.13}$$

$$h_j = \sum_i x_{ij} h_i^{\text{id}} + h_j^{\text{dep}}, \tag{B.14}$$

$$\log \varphi_{ij} = \frac{p\hat{b}_i}{RTB_j}\left(Z_j - 1\right) - \log\left(Z_j - B_j\right) - \frac{A_j}{B_j\sqrt{8}}\left(\frac{\frac{\partial A_j}{\partial x_{ij}}}{A_j} - \frac{p\hat{b}_i}{RTB_j}\right)\log\left(\frac{Z_j + (1+\sqrt{2})B_j}{Z_j + (1-\sqrt{2})B_j}\right). \tag{B.15}$$

Peng–Robinson departure functions are:

$$g_j^{\text{dep}} = \log\left(Z_j - B_j\right) - \frac{A_j}{B_j\sqrt{8}}\log\left(\frac{Z_j + (1+\sqrt{2})B_j}{Z_j + (1-\sqrt{2})B_j}\right), \tag{B.16}$$

$$h_j^{\text{dep}} = (Z_j - 1)RT + \frac{RT^2\frac{\partial A_j}{\partial T} + RTA_j}{B_j\sqrt{8}}\log\left(\frac{Z_j + (1+\sqrt{2})B_j}{Z + (1-\sqrt{2})B_j}\right). \tag{B.17}$$

For the evaluation of the ideal component-enthalpy h_i^{id}, heat capacity coefficients at constant pressure $c_{p,k}$ are given in Table B.3. For water and carbon dioxide it holds [1,2]

$$h_i^{\text{id}} = \sum_{k=1}^{4} c_{p,k}\left(T^k - T_{\text{ref}}^k\right), \tag{B.18}$$

and for hydrogen sulfide and nitrogen [30]

$$h_i^{\text{id}} = c_{p,1}\left(T - T_{\text{ref}}\right) + \frac{c_{p,2}}{2}\left(T^2 - T_{\text{ref}}^2\right) - c_{p,3}\left(T^{-1} - T_{\text{ref}}^{-1}\right). \tag{B.19}$$

The derivatives required to assemble the linearized System (3.3) are computed using PorePy's AD framework [34].

Remark. To avoid numerical instabilities caused by overflow errors, it is recommended to truncate log and exp using

$$\log_{trunc}(x) = \log(\max\{x, \epsilon\}),$$
$$\exp_{trunc}(x) = \exp(\min\{x, \log(N-1)\}),$$

with ϵ is a small number and N close to the largest number representable with the used float precision. This plays an important role in cases where Z approaches B, which is frequently encountered in the course of iterations.

References

[1] D. Zhu, R. Okuno, A robust algorithm for isenthalpic flash of narrow-boiling fluids, Fluid Phase Equilib. 379 (2014) 26–51, http://dx.doi.org/10.1016/j.fluid.2014.07.003.

[2] D. Zhu, R. Okuno, Analysis of narrow-boiling behavior for thermal compositional simulation, in: D. Zhu, R. Okuno (Eds.), SPE Reservoir Simulation Conference, Day 1 Mon, February 23, 2015, D011S001R002, URL: https://onepetro.org/spersc/proceedings/15RSS/1-15RSS/D011S001R002/183434.

[3] S. Saha, J.J. Carroll, The isoenergetic-isochoric flash, Fluid Phase Equilib. 138 (1) (1997) 23–41, http://dx.doi.org/10.1016/S0378-3812(97)00151-9.

[4] M.L. Michelsen, State function based flash specifications, Fluid Phase Equilib. 158 (1999) 617–626, http://dx.doi.org/10.1016/S0378-3812(99)00092-8.

[5] M.L. Michelsen, The isothermal flash problem. Part I. Stability, Fluid Phase Equilib. 9 (1982) 1–19, http://dx.doi.org/10.1016/0378-3812(82)85001-2.

[6] M.L. Michelsen, The isothermal flash problem. Part II. Phase-split calculation, Fluid Phase Equilib. 9 (1982) 21–40, http://dx.doi.org/10.1016/0378-3812(82)85002-4.

[7] D. Zhu, R. Okuno, Multiphase isenthalpic flash integrated with stability analysis, Fluid Phase Equilib. 423 (2016) 203–219, http://dx.doi.org/10.1016/j.fluid.2016.04.005.

[8] R. Okuno, R. Johns, K. Sepehrnoori, A new algorithm for Rachford-Rice for multiphase compositional simulation, SPE J. 15 (2) (2010) 313–325, http://dx.doi.org/10.2118/117752-PA.

[9] M. Connolly, H. Pan, M. Imai, H.A. Tchelepi, Reduced method for rapid multiphase isenthalpic flash in thermal simulation, Chem. Eng. Sci. 231 (2021) 116150, http://dx.doi.org/10.1016/j.ces.2020.116150.

[10] A. Lauser, C. Hager, R. Helmig, B. Wohlmuth, A new approach for phase transitions in miscible multi-phase flow in porous media, Adv. Water Resour. 34 (8) (2011) 957–966, http://dx.doi.org/10.1016/j.advwatres.2011.04.021.

[11] I. Ben Gharbia, M. Haddou, Q.H. Tran, D.T.S. Vu, An analysis of the unified formulation for the equilibrium problem of compositional multiphase mixtures, ESAIM: Math. Modell. Numer. Anal. 55 (2021) 2981–3016, http://dx.doi.org/10.1051/m2an/2021075.

[12] D.-Y. Peng, D.B. Robinson, A new two-constant equation of state, Ind. Eng. Chem. Fundam. 15 (1) (1976) 59–64, http://dx.doi.org/10.1021/i160057a011.

[13] A.K. Gupta, P. Bishnoi, N. Kalogerakis, Simultaneous multiphase isothermal/isenthalpic flash and stability calculations for reacting/non-reacting systems, Gas Sep. Purif. 4 (4) (1990) 215–222, http://dx.doi.org/10.1016/0950-4214(90)80045-M.

[14] C. Bell, Contributors, Thermo: Chemical properties component of chemical engineering design library (ChEDL), 2021, URL: https://github.com/CalebBell/thermo.

[15] M.L. Michelsen, J. Mollerup, Thermodynamic Modelling: Fundamentals and Computational Aspects, Tie-Line Publications, 2004.

[16] D.T.S. Vu, Numerical Resolution of Algebraic Systems with Complementarity Conditions : Application to the Thermodynamics of Compositional Multiphase Mixtures, No. 2020UPASG006 (Thesis), Université Paris-Saclay, 2020, URL: https://theses.hal.science/tel-02987892.

[17] D.T.S. Vu, I. Ben Gharbia, M. Haddou, Q.H. Tran, A new approach for solving nonlinear algebraic systems with complementarity conditions. Application to compositional multiphase equilibrium problems, Math. Comput. Simulation 190 (2021) 1243–1274, http://dx.doi.org/10.1016/j.matcom.2021.07.015.

[18] I. Ben Gharbia, J. Ferzly, M. Vohralík, S. Yousef, Semismooth and smoothing Newton methods for nonlinear systems with complementarity constraints: Adaptivity and inexact resolution, J. Comput. Appl. Math. 420 (2023) 114765, http://dx.doi.org/10.1016/j.cam.2022.114765.

[19] M.H. Wright, The interior-point revolution in optimization: History, recent developments, and lasting consequences, Bull. Amer. Math. Soc. 42 (1) (2005) 39–56, URL: https://www.ams.org/journals/bull/2005-42-01/S0273-0979-04-01040-7/.

[20] H.H. Rachford, J. Rice, Procedure for use of electronic digital computers in calculating flash vaporization hydrocarbon equilibrium, J. Pet. Technol. 4 (10) (1952) 19–3, http://dx.doi.org/10.2118/952327-G.

[21] C.H. Whitson, M.L. Michelsen, The negative flash, Fluid Phase Equilib. 53 (1989) 51–71, http://dx.doi.org/10.1016/0378-3812(89)80072-X.

[22] M.L. Michelsen, Multiphase isenthalpic and isentropic flash algorithms, Fluid Phase Equilib. 33 (1987) 13–27, http://dx.doi.org/10.1016/0378-3812(87)87002-4.

[23] J.O. Valderrama, The state of the cubic equations of state, Ind. Eng. Chem. Res. 42 (8) (2003) 1603–1618, http://dx.doi.org/10.1021/ie020447b.

[24] J.S. Lopez-Echeverry, S. Reif-Acherman, E. Araujo-Lopez, Peng-robinson equation of state: 40 years through cubics, Fluid Phase Equilib. 447 (2017) 39–71, http://dx.doi.org/10.1016/j.fluid.2017.05.007.

[25] F. Maxim, C. Contescu, P. Boillat, B. Niceno, K. Karalis, A. Testino, C. Ludwig, Visualization of supercritical water pseudo-boiling at Widom line crossover, Nature Commun. 10 (1) (2019) 4114, http://dx.doi.org/10.1038/s41467-019-12117-5.

[26] A. Lamorgese, W. Ambrosini, R. Mauri, Widom line prediction by the Soave-Redlich-Kwong and Peng-Robinson equations of state, J. Supercrit. Fluids 133 (2018) 367–371, http://dx.doi.org/10.1016/j.supflu.2017.07.031.

[27] M. Castier, Solution of the isochoric–isoenergetic flash problem by direct entropy maximization, Fluid Phase Equilib. 276 (1) (2009) 7–17, http://dx.doi.org/10.1016/j.fluid.2008.10.005.

[28] B. Sanjuan, R. Millot, C. Innocent, C. Dezayes, J. Scheiber, M. Brach, Major geochemical characteristics of geothermal brines from the upper rhine graben granitic basement with constraints on temperature and circulation, Chem. Geol. 428 (2016) 27–47, http://dx.doi.org/10.1016/j.chemgeo.2016.02.021.

[29] I. Søreide, C.H. Whitson, Peng-robinson predictions for hydrocarbons, CO2, N2, and H2S with pure water and NaCI brine, Fluid Phase Equilib. 77 (1992) 217–240, http://dx.doi.org/10.1016/0378-3812(92)85105-H.

[30] N. de Nevers, Appendix A: Useful tables and charts, in: Physical and Chemical Equilibrium for Chemical Engineers, John Wiley & Sons, Ltd, 2012, pp. 303–317, http://dx.doi.org/10.1002/9781118135341.app1.

[31] A. Mitsos, P.I. Barton, A dual extremum principle in thermodynamics, AIChE J. 53 (8) (2007) 2131–2147, http://dx.doi.org/10.1002/aic.11230.
[32] D. Jungen, H. Djelassi, A. Mitsos, Adaptive discretization-based algorithms for semi-infinite programs with unbounded variables, Math. Methods Oper. Res. 96 (1) (2022) 83–112, http://dx.doi.org/10.1007/s00186-022-00792-y.
[33] S. Chabab, J.L. Cruz, M. Poulain, M. Ducousso, F. Contamine, J.P. Serin, P. Cézac, Thermodynamic modeling of mutual solubilities in gas-laden brines systems containing CO2, CH4, N2, O2, H2, H2O, NaCl, CaCl2, and KCl: Application to degassing in geothermal processes, Energies 14 (17) (2021) http://dx.doi.org/10.3390/en14175239.
[34] E. Keilegavlen, R. Berge, A. Fumagalli, M. Starnoni, I. Stefansson, J. Varela, I. Berre, PorePy: An open-source software for simulation of multiphysics processes in fractured porous media, Comput. Geosci. 25 (2021) 243–265, http://dx.doi.org/10.1007/s10596-020-10002-5.